Chemosphere 360 (2024) 142347

Contents lists available at ScienceDirect

Chemosphere

journal homepage: www.elsevier.com/locate/chemosphere

Progress in membrane distillation processes for dye wastewater treatment: A review

Lebea N. Nthunya [a,*], Kok Chung Chong [b,c], Soon Onn Lai [b,c], Woei Jye Lau [d], Eduardo Alberto López-Maldonado [e], Lucy Mar Camacho [f], Mohammad Mahdi A. Shirazi [g], Aamer Ali [g], Bhekie B. Mamba [h], Magdalena Osial [i], Paulina Pietrzyk-Thel [i], Agnieszka Pregowska [i], Oranso T. Mahlangu [h,**]

[a] Molecular Sciences Institute, School of Chemistry, University of the Witwatersrand, Private Bag X3, 2050, Johannesburg, South Africa
[b] Department of Chemical Engineering, Lee Kong Chian Faculty of Engineering and Science, Universiti Tunku Abdul Rahman, Jalan Sungai Long, Kajang 43000, Selangor, Malaysia
[c] Centre of Photonics and Advanced Materials Research, Universiti Tunku Abdul Rahman, Kampar 31900, Perak, Malaysia
[d] Advanced Membrane Technology Research Centre (AMTEC), Faculty of Chemical and Energy Engineering, Universiti Teknologi Malaysia, Johor Bahru 81310, Johor, Malaysia
[e] Faculty of Chemical Sciences and Engineering, Autonomous University of Baja California, 22424, Tijuana, B.C., Mexico
[f] Department of Environmental Engineering, Texas A&M University-Kingsville, MSC 2013, 700 University Blvd., Kingsville, TX 78363, USA
[g] Centre for Membrane Technology, Department of Chemistry and Bioscience, Aalborg University, Fredrik Bajers Vej 7H, 9220 Aalborg, Denmark
[h] Institute for Nanotechnology and Water Sustainability, College of Science, Engineering and Technology, University of South Africa, Florida Science Campus, 1709 Roodepoort, South Africa
[i] Institute of Fundamental Technological Research, Polish Academy of Sciences, Pawińskiego 5B, 02-106 Warsaw, Poland

HIGHLIGHTS

- Discharge of dye effluent requires robust and cost-effective treatment processes.
- Membrane distillation emerged as a promising tool towards dye remediation.
- The current study reviewed research advancement towards environmental dye remediation.
- However, fouling and thermal efficiency of MD remain a major challenge.
- The reviewed study suggested optimization of membrane and module designs for effective dye remediation.

GRAPHICAL ABSTRACT

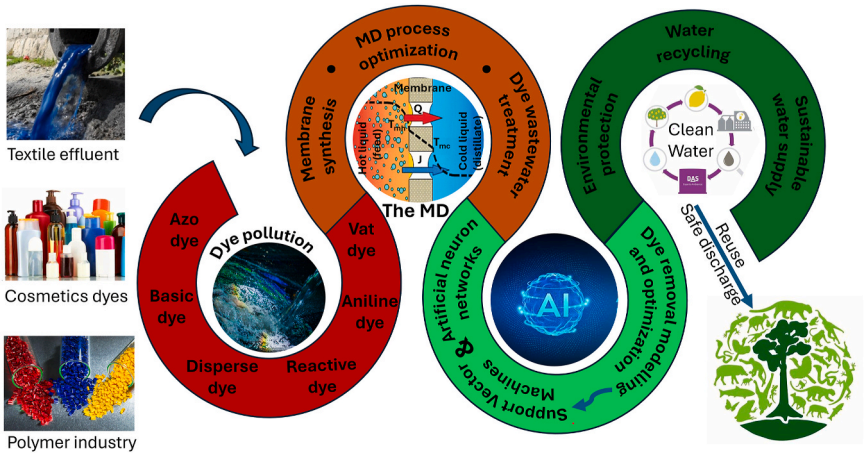

* Corresponding author.
** Corresponding author.
E-mail addresses: nthunyalebea@gmail.com (L.N. Nthunya), mahlaot@unisa.ac.za (O.T. Mahlangu).

https://doi.org/10.1016/j.chemosphere.2024.142347
Received 11 March 2024; Received in revised form 26 April 2024; Accepted 14 May 2024
Available online 15 May 2024

ARTICLE INFO

Keywords:
Energy consumption
Dye effluent
Fouling
Heat and mass transfer
Membrane and module design
Membrane distillation

ABSTRACT

Textile and cosmetic industries generate large amounts of dye effluents requiring treatment before discharge. This wastewater contains high levels of reactive dyes, low to none-biodegradable materials and chemical residues. Technically, dye wastewater is characterised by high chemical and biological oxygen demand. Biological, physical and pressure-driven membrane processes have been extensively used in textile wastewater treatment plants. However, these technologies are characterised by process complexity and are often costly. Also, process efficiency is not achieved in cost-effective biochemical and physical treatment processes. Membrane distillation (MD) emerged as a promising technology harnessing challenges faced by pressure-driven membrane processes. To ensure high cost-effectiveness, the MD can be operated by solar energy or low-grade waste heat. Herein, the MD purification of dye wastewater is comprehensively and yet concisely discussed. This involved research advancement in MD processes towards removal of dyes from industrial effluents. Also, challenges faced by this process with a specific focus on fouling are reviewed. Current literature mainly tested MD setups in the laboratory scale suggesting a deep need of further optimization of membrane and module designs in near future, especially for textile wastewater treatment. There is a need to deliver customized high-porosity hydrophobic membrane design with the appropriate thickness and module configuration to reduce concentration and temperature polarization (CP and TP). Also, energy loss should be minimized while increasing dye rejection and permeate flux. Although laboratory experiments remain pivotal in optimizing the MD process for treating dye wastewater, the nature of their time intensity poses a challenge. Given the multitude of parameters involved in MD process optimization, artificial intelligence (AI) methodologies present a promising avenue for assistance. Thus, AI-driven algorithms have the potential to enhance overall process efficiency, cutting down on time, fine-tuning parameters, and driving cost reductions. However, achieving an optimal balance between efficiency enhancements and financial outlays is a complex process. Finally, this paper suggests a research direction for the development of effective synthetic and natural dye removal from industrially discharged wastewater.

List of Acronyms

ANNs	Artificial neuron networks	PEI	Polyetherimide
AGMD	Air gap membrane distillation	PES	polyether sulfone
AgNPs	Silver nanoparticles	pH_{pzc}	Point of zero charge
AI	Artificial Intelligence	PP	Polypropylene
CFD	Computational fluid dynamics	PS	Polystyrene
CI	Colour index	PTFE	Polytetrafluoroethylene
CNTs	Carbon nanotubes	PU	Polyurethane
CP	Concentration polarization	PVA	Poly(vinylalcohol)
CR	Congo red dye	PVDF	Polyvinylidene fluoride
DCMD	Direct contact membrane distillation	PVDF-HFP	Poly(vinylidene fluoride-co-hexafluoropropene)
HFP	Hexafluoropropylene	SAN	Styrene acrylonitrile
HIPS	High-impact polystyrene	SBMA	Sulfobetaine methacrylate
LEP	Liquid entry pressure	SGMD	Sweeping gas membrane distillation
MB	Methylene blue dye	SiO_2	Silica
MD	Membrane distillation	SVM	Support vector machine
MGMD	Material gap membrane distillation	TiO_2	Titanium dioxide
MO	Methyl orange dye	TP	Temperature polarization
PDMS	Polydimethylsiloxane	VMD	Vacuum membrane distillation
PEG	Polyethylene glycol	Zn $(CH_3CO_2)_2$	Zinc acetate

1. Introduction

Rapid progress of industrialization affects the water quality, resulting in an increasing freshwater crisis globally (Katheresan et al., 2018). Inadequate treatment of wastewater leads to various chemical release to the environment, where large group of industrial waste contains dyes. These compounds are classified according to their chromophore structure, colour index (CI), and its application (Benkhaya et al., 2020a; Rauf and Hisaindee, 2013). Classification of chromophore structure is based on functional groups of the dye molecule. This include acridine, anthraquinone, azo, cyanine, diarylmethane, indigoid, nitro, nitroso, oxazine, phthalein, quinone-imine, triarylmethane, triphenylmethane, xanthene (Benkhaya et al., 2020b; Raman and Kanmani, 2016). On one hand, CI classification includes over 8000 synthetic dyes with various names used in industrial applications. Depending on the textile type, different dyes are commonly used, e.g., sulphur (Nguyen and Juang, 2013), reactive (Zhang et al., 2005; Pei et al., 2017), cationic (Benkhaya et al., 2020a; Xiao et al., 2017), and azoic dyes (Hassan and Carr, 2018). These dyes are used to colourize cotton, silk, wool, nylon, rayon, viscose, cellulose acetate, paper, polyester, leather, acrylic, and synthetic fibres. Owing to their extensive use in textile, pharmaceutics, rubber, paint, food, cosmetic, paper, and pulp industries, dyes are released to the water streams causing severe environmental pollution. Textiles processing require several steps, namely, bleaching, mercerization, printing, and finishing. These steps require large amount of water (Rajkumar and Kim, 2006). For instance, bleaching process requires treatment with either reducing or oxidizing agents to get rid of the dye. In mercerization, the material is treated with specific chemicals to improve its strength and affinity to dyes. The finishing process towards the transformation of the fabrics into functional material like waterproofing, glazing, sizing, and smoothing generates huge quantities of wastewater containing dyes (Holkar et al., 2016).

Despite wide use of dyes in many fields, they are known for their adverse health effect. Literature reported an increased cancer appearance linked to textile industry proximity (Serra et al., 2008; Singh and Chadha, 2016). Also, hairdressers exposed to oxidative hair dyes are diagnosed with respiratory health problems (Helaskoski et al., 2014). The release of dyes to the aquatic environment does not only affect human beings but also deteriorate water quality, affecting the level of dissolved oxygen. Moreover, dyes undergo chemical reactions exacerbating their environmental toxicity. Acute, chronic, or cytotoxic effect of dyes has been broadly reported in algae, bacteria, fish, and mice (Fried et al., 2022). Other studies reported dye toxicity on brain, kidney, liver, heart, and other organs as well as respiratory, hormonal, and immune systems (Rovira and Domingo, 2019; Kant, 2012).

To minimize the adverse effects of dye wastewater, various physicochemical methods have been extensively used to treat it (Fig. 1). Physical treatment processes include adsorption, ion exchange, and membrane technologies. These techniques are easy to use, economical, and chemical-free (Al-Tohamy et al., 2022). However, physical processes produce high amounts of sludge and are limited towards treatment of dye-containing wastewater. On one hand, various chemical

processes including advanced oxidative processes (AOP), photocatalysis, and electrocoagulation have been extensively evaluated to treat the dye wastewater. Although they remove dyes from harsh operating conditions and generate less sludge, they are pH dependent, expensive and form undesirable by-products. Similarly, electrochemical processes produce no sludge and do not require use of chemicals. However, it is costly and less effective compared to other technologies.

Biological processes have also been used extensively to treat dye-containing wastewater. This involves enzyme, algae, yeast, bacterial, and fungal assisted processes (Al-Tohamy et al., 2022). Biological processes avoid chemical usage and produce no sludge. However, their efficiency is dependent on the water chemistry including pH fluctuations and other conditions inhibiting activity of the biological agents. The publication record (in the past 10 years since 2013) of the dye wastewater treatment is presented in Fig. 1a. It is important to note that no single dye wastewater treatment process is the most suitable technology due to various advantages and drawbacks (Samsami et al., 2020). For instance, the complex nature of the dye wastewater hinders satisfactory treatments meeting regulatory standards upon use of the mentioned technologies. This necessitates the combination of various technologies towards production of high-quality water. However, membrane distillation (MD) emerged as a promising technology, capable of producing high-quality water from dye wastewater. The publication growth record of dye wastewater treatment through MD is presented in Fig. 1b. The number of publications for dye wastewater treatment via all methods increased from 10,904 in 2013 to 46,884 in 2023. The total number of publications between 2013 and 2023 was 27,5431. This was a tremendous increase, indicating the research interests of this topic. In the case of dye wastewater treatment via MD, the publications increased from 677 in 2023 to 3910 in 2023. The total number of publications between 2013 and 2023 was 21,105. Such developments demonstrate the capability of this technology in treating the dye-polluted wastewater.

The first generation of MD research used commercially available hydrophobic membranes for wastewater treatment (Khayet, 2011; Shirazi and Kargari, 2015). For example, the first report on the application of MD textile wastewater treatment date back in 1991, where the authors used commercial hollow fibre membranes made of polypropylene (PP) to treat synthetic wastewater by direct contact membrane distillation (DCMD) (Drioli and Matera, 1991). However, these membranes were not specifically fabricated for MD, thus presenting impaired performance as per reported permeate flux and energy efficiency. This is more challenging in case of textile wastewater treatment containing organic and inorganic dyes and other chemicals (Banat et al., 2005a; Criscuoli et al., 2008a). Therefore, the next generation of MD research for textile wastewater considered the fabrication of specific membranes for this application, particularly focusing on membrane fouling and operating conditions (Mpala et al., 2024; Ramlow et al., 2019a; Leaper et al., 2019; Laqbaqbi et al., 2019a). This involved employing hydrophobic polymers to produce wetting resistant membranes. The most studied polymers are polypropylene (PP), polyvinylidene fluoride (PVDF), polytetrafluoroethylene (PTFE), and polyethylene (PE) whose chemical structures are provided in Fig. 2. The membranes prepared from these polymers are not wetted by process liquids, thus facilitating the mass transfer through passage of the water vapour through the porous membrane. Other polymers evaluated in MD systems include HIPS and PDMS due to their hydrophobic nature. Although hydrophobic polymers presented fascinating results, they are increasingly modified to produce various novel polymer types for use in MD. These new generation of hydrophobic polymers are poly (ethene-co-chlorotrifluoroethene) (ECTFE), poly(vinylidene fluoride-co-tetrafluoroethylene) (PVDF-co-TFE), poly(vinylidene fluoride-co-tetrafluoroethylene) (PVDF-co-TFE), poly(vinylidene fluoride-co-chlorotrifluoroethylene) (PVDF-co-CTFE), and poly (tetrafluroethylene-co-hexafluoropropylene) (FEP) (Eykens et al., 2017). The membrane synthesis from these polymers is still at development stage of research, thus requiring intensive optimization process to improve the MD process performance. Among the first attempts, Mokhtar et al. (2014) fabricated PVDF hollow fibre membranes with varying polymer concentrations (12–18 wt%) for use in dye effluent treatment (Mokhtar et al., 2014a). As per reported findings, 12 wt% polymer concentration, with 0.14 μm pore size and 450 kPa liquid entry pressure (LEP) provided excellent performance in terms of permeate flux (~5 kg m^{-2} h^{-1}) and dye rejection (>99.80%). Also, fouling behaviour of developed hollow fibre membrane was evaluated in a 40-h operation, presenting 50% flux decline (Mokhtara et al., 2016).

Despite progressive reports on MD applications towards treatment of dye effluents, there are limited review studies focusing on the subject matter. In their recent review study, Suresh et al. (2023) reported

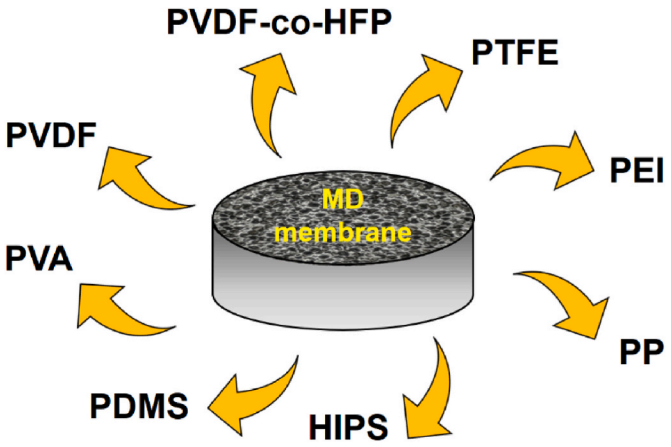

Fig. 2. The commonly used polymers in MD processes.

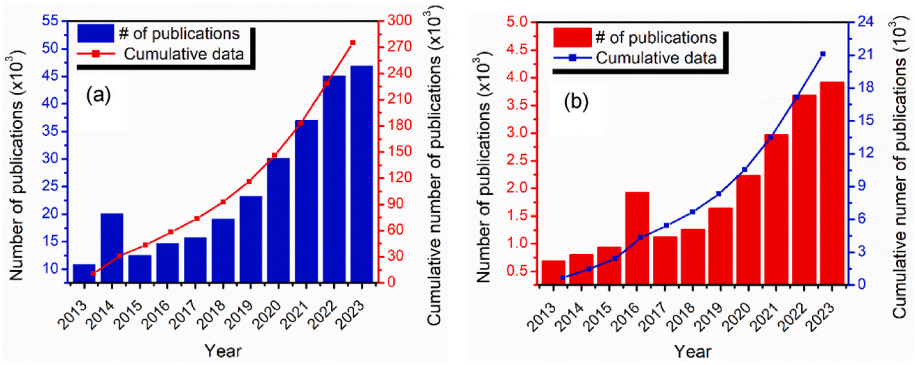

Fig. 1. Number of publications related to dye wastewater treatment for the past ten years, (a) general treatment methods and (b) MD technologies. The data was retrieved from Scopus.

various membrane applications processes including adsorption, filtration, catalysis (oxidant activation, ozonation, Fenton process, and photocatalysis) and MD towards removal of synthetic dye from wastewater (Suresh et al., 2023). Besides dye treatment, MD is a viable technology for seawater desalination because it can process high-salinity water (Chimanlal et al., 2023a). However, MD application is limited by low vapour flux and fouling – an inherent challenge in all membrane processes. One of the approaches to overcome these challenges is to make superhydrophobic membranes (Chimanlal et al., 2023b). This this is achieved through the incorporation of inorganic nanomaterials such as graphene-based materials, carbon nanotubes (CNTs), metal-oxide nanoparticles (MNPs), clays as well as zeolitic imidazolate frameworks (ZIFs) (Lousada et al., 2023; Gontarek-castro et al., 2022). Membrane wetting is another challenge associated with MD. Fouling and wetting in MD leads to immediate failure in membrane separation (Mahlangu et al., 2024). Therefore, it is important to understand fouling and wetting mechanisms in MD during treatment of various feed streams of different physicochemical properties (Gontarek-castro and Castro-muñoz, 2023). The MD membranes are generally prepared from non-biodegradable polymers, harmful solvents and fluoroalkyl silanes. A recent review debates some inspiration for the fabrication of the next generation of MD membranes using greener approaches (Gontarek-castro and Castro-Munoz, 2024). These membranes have potential for commercialization.

Some major drawbacks encountered with polymeric membranes is achieving high permeability and selectivity simultaneously (Zamidi et al., 2021). Highly permeable membranes often have low permeability and vice versa. However, recent advancements have led to the formation of ultrathin membranes, breaking the trade-off between selectivity and permeance (Zamidi et al., 2022). This is due to the ultrathin nature of the selective layer and lack of defects in the membrane structure. Several approaches including atomic layer deposition, in situ crystal formation, interfacial polymerization, Langmuir–Blodgett technique, facile filtration process, and gutter layer formation have been used to prepare membranes with high selectivity and permeability. These procedures take advantage of the intrinsic nature of nanostructured materials such as polymers, zeolites, covalent–organic frameworks, metal–organic frameworks, and graphene to prepare membranes for various applications in liquid separation – a focus of this study. Detailed overview of these techniques can be found in the literature (Roberto et al., 2020). Chemical grafting or crosslinking of polyimide chains are other strategies adopted to improve selectivity and specific permeance. However, the separation efficiency often improves at the expense of fluid permeability as the degree of crosslinking increases (Ahmad et al., 2018). Similarly, non-selective filler-polymer interfacial voids reduce selectivity of mixed matrix membranes (Jain et al., 2021).

Besides tremendous progress in the configuration of MD systems, there are many problems limiting its performance on a broad scale, requiring critical attention. The most challenging issues in addition to wetting and fouling affecting membrane flux and separation efficiency include high-energy consumption, long time of operation, and membrane regeneration. The current review reported different aspects and recent solutions in the effective MD process focusing on the main configurations used in laboratory and industrial scale, where considerable research articles focus on the commercial membranes. Although the MD is a promising technology, its effectiveness depends on several features including operation parameters like feed temperature, flowrate, feed concentration; physicochemical properties of the membrane (pore size and porosity, permeability, membrane thickness, hydrophobicity, thermal stability, polymer type used for membrane fabrication, and the MD system configuration. The current literature mainly tested MD setups in the laboratory scale suggesting a deep need for further optimization of membrane and module designs in near future, especially for textile wastewater treatment. There is a need to deliver customized high-porosity hydrophobic membrane design with the appropriate thickness and module configuration to reduce concentration and temperature polarization (CP and TP), minimize waste energy and increase MD efficiency and water recovery. More research should optimize configurations and re-design the membranes by incorporating new materials (e.g. hollow fibres, nanofibres, and nanomaterials) to enhance the fluid dynamics, reduce waste energy, and improve re-use of membranes and versatility to deal with industrial dye effluents. To increase the operation scale of MD, more mitigation and cost-effective antifouling strategies should be implemented.

Among practical aspects, the theoretical studies are widely implemented to enhance MD technology. The artificial intelligence (AI)-based methods enable optimization of the input variables to achieve the highest efficiency of the dye removal (maximize the removal value). The key issue for developing efficient AI-based solutions is to provide the developers with large and good quality data. AI-based algorithms can increase the efficiency of the entire process, shortening its duration, optimizing its parameters, and reducing costs. Advanced machine learning techniques can support the development of the MD scale processes. However, this field of research is still poorly explored in textile wastewater treatment and need more modelling studies including correlation between the membrane and module design, and mechanism of fouling and wetting. These aspects are comprehensively and concisely addressed in this review, with the strategy of ensuring improved MD process performance in textile industry.

2. Membrane development for textile and dye wastewater treatment

Membrane development characterized by fouling and scaling resistance is a promising approach towards treatment of dye wastewater in MD. For example, An et al. (2017) fabricated a novel nanofibre membrane by incorporating polydimethylsiloxane (PDMS) onto a electrospun poly(vinylidene fluoride-co-hexafluoropropene) (PVDF-HFP) membrane (An et al., 2017). The new hybrid membrane exhibited a notable decrease in surface energy, as seen by the contact angle measurement of 155.4°. Additionally, the membrane displayed high surface roughness (R_a = 1285 nm). The zeta potential of the new membrane exhibited a more pronounced negative value compared to a commercial PVDF membrane. As per authors argument, the new membrane exhibited wetting resistance and antifouling qualities during treatment of dye wastewater with varying charges. This resulted in the formation of a flake-like structure of dye-dye interactions on the surface of the membrane, rather than within its pores. Furthermore, this phenomenon resulted in a notable increase in the productivity of the new nanofibre membrane, reaching a permeate flux of 34 L m^{-2} h^{-1}, which is 50% greater compared to the productivity of the commercial membrane.

Pore wetting is another major challenge of MD, demonstrating a direct collapse of the membrane performance (Shirazi et al., 2014). During treatment of textile wastewater, chemicals and surfactants increase the pore wetting risk (Yang et al., 2021). García et al. (2018) used a custom-made PTFE membrane coated by hydrophilic polyurethane (PU) in a pilot scale DCMD system (García et al., 2018). The system was developed to treat textile wastewater containing surfactant. Authors reported increased wetting of the commercial PTFE membrane as evidenced by increase in the permeate conductivity. In contrast, the hydrophilic-coated membrane exhibited a consistent decrease in permeate conductivity, indicating the presence of a wetted membrane. Despite the favorable outcome, the coated membrane did not withstand a routine cleaning procedure including washing by sodium hydroxide (NaOH) aqueous solution, which is commonly employed in membrane processes.

Similar to other properties, MD performance is affected by membrane porosity. In fact, high porosity is required to transfer the vapour molecules. This achieved by new fabrication techniques for highly porous, flat sheet membranes, such as electrospinning (Nthunya et al., 2019a, 2019b). Shirazi et al. (2020) developed a durable membrane with a dual-layer structure and exceptional characteristics for treatment

of industrial dye wastewater (Shirazi et al., 2020a). This nanofibre membrane possessed a composite structure consisting of the cost-effective styrene acrylonitrile (SAN) polymer as the top layer, alongside a commercially available hydrophilic nonwoven material for the supporting layer. As per reported findings, the approach presented potential commercialization of the DCMD process in the treatment of high-temperature dye wastewater. The nanofibre membrane exhibited notable characteristics compared to a commercial PTFE membrane, including a high hydrophobicity (≥148°), increased porosity (≥81%), and a reduced tortuosity factor (1.71). All these led to a superior performance of membrane, precisely, 28.31 kg m^{-2} h^{-1} permeate flux and a commendable rejection rate of 98.2%. In their study, Khoshnevisan and Bazgir (2020) examined a hot-pressed nanofibre membrane made of HIPS towards treatment of textile wastewater at different concentrations (Shirazi et al., 2020a). The hot-press post treatment of the membrane samples enhanced mechanical strength with an improvement in pore size distribution and LEP. The dye rejection of the DCMD process exceeded 99.8% when varying amounts of dye were utilized as the feed. However, the membranes were fouled at high dye concentrations. Yadav et al. (2021) developed an innovative mixed matrix membranes, including MIL101(Fe) impregnated into PVDF-HFP (Yadav et al., 2021a). The membrane composed of 20% PVDF-HFP and 0.5% MIL101 (Fe) presented >98% dye removal along with 6.75 L m^{-2} h^{-1} permeate flux.

Photocatalytic MD membranes emerged as a promising self-healing to improve process performance. For example, Huang et al. (2017) fabricated photocatalytic membrane with highly porous structure by sintering electrospun composite membranes consisting of PTFE, poly (vinylalcohol) (PVA), and zinc acetate ($Zn(CH_3CO_2)_2$) (Huang et al., 2017). The resulting membranes were supported by a substrate of zinc oxide (ZnO). According to the findings, the spinning solution displayed favorable electrospinning characteristics, while the membranes exhibited remarkable flexibility, elevated chemical stability, and large specific surface area. The authors applied their PTFE/ZnO membranes in vacuum membrane distillation (VMD) through the implementation of photo-degradation tests towards efficiency evaluation. According to the obtained results, the trials using photo-degradation yielded a notable 99.7% salt rejection. In addition, the PTFE/ZnO membranes exhibited favorable self-cleaning capabilities. According to reported findings, the used membranes presented 94.1% flux recovery following a 3-h period of UV irradiation cleaning (Fig. 3).

In addition to flat sheet membranes, research is geared towards preparation of hollow fibre membranes for textile wastewater treatment. Li et al. (2019) used the dilute solution coating technique to manufacture hydrophobic PVDF hollow fibre composite membranes (Li and Feng, 2019). The process was aimed at fabricating a specific surface structure analogous to the dual micro-nano structure, mimicking the properties of a lotus leave. This preparation procedure increased the surface contact angle of the membrane from 93.6° to 130.8°. The fabricated membranes were evaluated towards separation of congo red and methylene blue dyes from synthesized wastewater using VMD. The findings reported an increase in permeate flux and dye rejection (>99%) in comparison with the control PVDF membrane. In another work, Mousavi et al. (2021) modified a hydrophobic polyetherimide (PEI) hollow fibre membrane through a dip-coating technique (Mousavi et al., 2021a). The authors coated the membranes using 2-(perfluoroalkyl) ethanol (Zonyl® BA). The prepared membranes were evaluated to remove methylene blue from a synthesized wastewater stream via air gap membrane distillation (AGMD). During a 76-h experiment, the developed hollow fibre membrane exhibited a permeate flux of 6.5 kg m^{-2}·h^{-1} and a methylene blue rejection of 98%.

In a recent work, Xie et al. (2023) fabricated a superhydrophobic PVDF membrane using a spray-coating technique with fluorinated silica nanoparticles (SiO_2 NPs) (Fig. 4) for the treatment of saline dye wastewater (Xie et al., 2023). The authors performed a detailed investigation on the effects of various operating variables (i.e., temperature difference, feed flowrate, salt concentration, dye concentration, and dye species) in DCMD. According to the research findings, the prepared superhydrophobic membrane presented a remarkable resistance to wetting and fouling with 99.9% salt and dye rejection. Additionally, the superhydrophobic membrane exhibited a notable water recovery rate of 90%. However, the authors reported a marginal 13.4% decrease in the permeate flux during a 39-h DCMD evaluation.

In the preparation of polymer-based ultrafiltration (UF)/nanofiltration (NF) membranes for MD, recent trends adopted greener approaches involving utilization of green solvents in membrane fabrication. Various polymeric membranes have been prepared via these green synthesis methods, and they include porous Matrimid® 5218 membranes (Russo et al., 2019) and NF membranes based on polyamide-cellulose acetate (Ounifi et al., 2022). Similarly, the preparation of green nanofillers and their incorporation into polymeric NF membranes has been reported. A recent comprehensive review discusses recent and ongoing progress on novel nanocomposite membranes based on green approaches for heavy metals removal from water (Loreti and Castro-mu, 2021). The membranes with green nanofillers improved hydrophilicity, water permeability and pollutant rejection capability. These membranes present fouling resistance and can be used for a lengthy period without degradation.

Table 1 provides a summary of the MD application towards dye removal from textile effluents. Among the MD configurations, the most popular design is DCMD owing to its simplicity in setup and low capital cost (Rovira and Domingo, 2019). In DCMD, both the feed and permeate solutions are in direct contact with the membrane at different interfaces. The temperature difference between the two membrane interfaces creates a partial vapour, facilitating the mass transfer from the feed to the permeate. Although the DCMD is known to be simple to design and

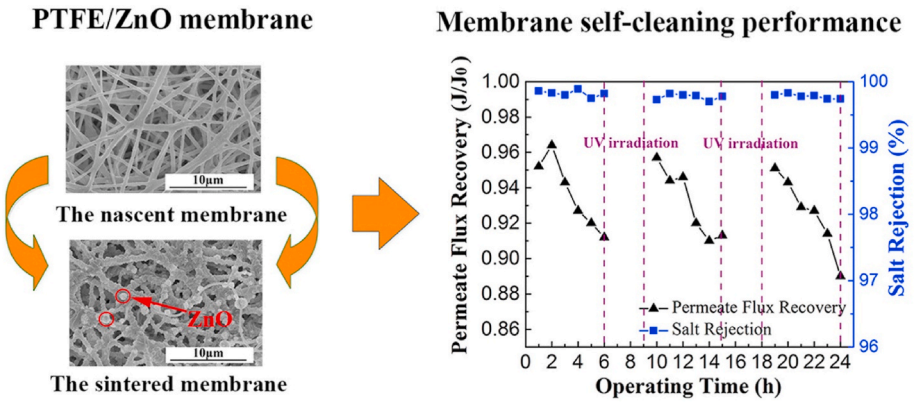

Fig. 3. The nanofibre PTFE/ZnO porous membrane with a self-cleaning mechanism for dye removal by VMD (Li et al., 2019).

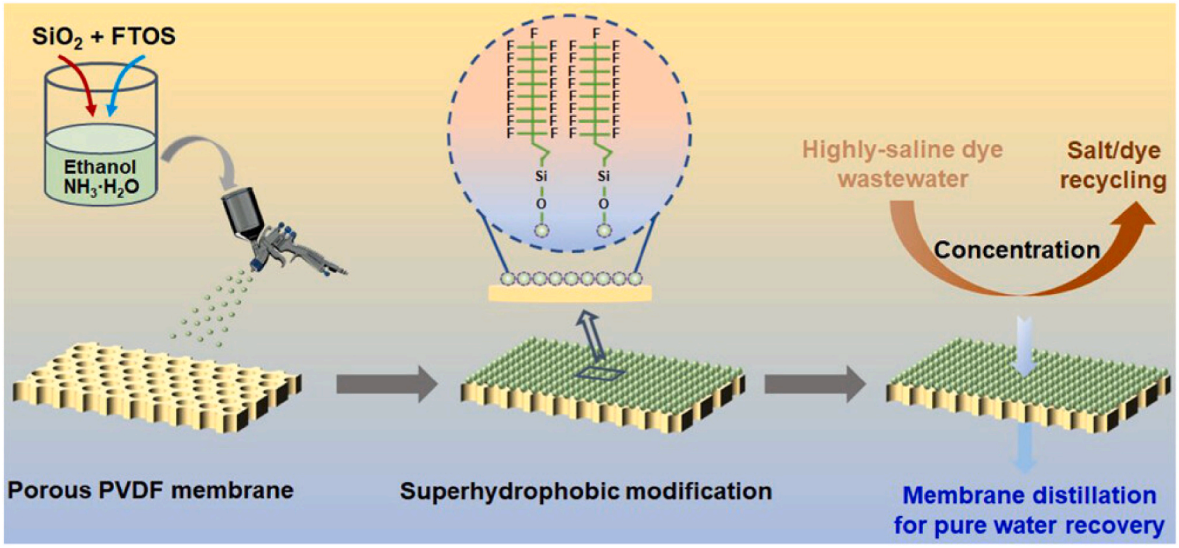

Fig. 4. Procedural fabrication of superhydrophobic SiO_2/PVDF membrane for dye removal from a highly saline wastewater (Xie et al., 2023).

operate, it experiences high conductive heat loss and thermal energy inefficiencies (Parani and Oluwafemi, 2021). To minimize the heat loss in MD processes, the VMD was proposed. In this configuration, the membrane is placed between the hot feed and the vacuum chamber (Zhang et al., 2013). The water vapour condensers outside the module in an external condenser. Although the VMD is thermally efficient, it is affected by membrane wetting due to high pressure differences resulting in low separation efficiencies (Izquierdo-Gil and Jonsson, 2003). Similarly, the cold inert gas is used to sweep the water vapour from to the external condenser, giving rise to SGMD. This configuration is thermally efficient (Said et al., 2020). However, it requires large condensers, thus making it expensive. In addition to SGMD, the AGMD was introduced, presenting high thermal efficiency influenced by reduced heat loss. In this configuration, the membrane is placed between the hot feed solution and the stagnant air (Nthunya et al., 2019b). The water vapour passes through the porous membrane and stagnant air to the condensing plate. This configuration faces mass transfer resistance resulting in low permeate flux (Parani and Oluwafemi, 2021). All these configurations require hydrophobic membranes to operate effectively. Commonly used membrane materials for MD processes are PTFE, PVDF, and PP. The choice of these polymeric materials involves their outstanding properties namely, high hydrophobicity, low surface energy, low melting point, high tolerance to oxidizing agents, and good thermal stability (Kant, 2012). From Table 1, dyes such as reactive orange, reactive blue, reactive black, methylene blue, and congo red are commonly used to evaluate the performance of membrane during MD processes with the operating feed and permeate temperatures 40–80 °C and 10–20 °C, respectively. As per reported findings, the permeate flux deteriorated as a function of time, mainly due to the surface fouling caused by dye adsorption/deposition.

3. Membrane fouling in textile/cosmetic wastewater

Fouling remains a major drawback in the application of membranes in liquid separations (Mahlangu et al., 2023a). Fouling does not only deteriorate membrane performance, but also increases operational costs due to requirements of frequent cleaning and membrane replacement (Nthunya et al., 2022). Membrane fouling is governed by various factors (Mahlangu et al., 2015). Various strategies are adopted to alleviate fouling in hydraulic- (NF/RO), osmotic- (FO) and vapour-pressure (MD) driven membranes (Mahlangu et al., 2024). Some of the strategies used to prevent fouling include the incorporation of nanofillers to prepare high performance and stable membranes (Salehi and Castro-mu, 2023; Cosme and Castro-mun, 2023). Nanofiller addition increases electron donor or Lewis base components of the membranes, thus reducing membrane-foulant affinity interactions (Mahlangu et al., 2023b). Subsequently, reversible fouling ratio contributes more to the observed total fouling ratio (Salehi and Castro-mu, 2023; Mahlangu et al., 2023b). Other modification processes include polymer blending, nanocomposite materials and chemical modification (Pichardo-romero et al., 2020). Also, alternative novel approaches used to combat biofouling include the addition of bacteriophages as biocidal agents, quorum quenching, advanced oxidation processes, and addition of metazoans amongst others (Mpala et al., 2022).

Inorganic dyes present in textile and cosmetic wastewater can potential cause membrane fouling of MD systems. During the MD process, only water molecules (vapour) pass through the hydrophobic membrane while non-volatile dye molecules are rejected by the membrane. As a result, the dye concentration adjacent to the membrane surface is gradually increased, causing concentration polarization (CP) (Du et al., 2023). Furthermore, high dye concentrations near the membrane surface develop a cake layer, leading to a significant increase in membrane transport resistance and reduction in permeate flux. By increasing the dye concentration in the feed solution from 50 ppm to 1000 ppm, Mokhtar et al. (2015) reported a gradual decline in permeate flux from ~10 kg $m^{-2}{\cdot}h^{-1}$ to 6.5 kg $m^{-2}{\cdot}h^{-1}$ when tested under hot and cold solution temperature of 70 °C and 20 °C, respectively (Mokhtar et al., 2015). The flux decline at high solute concentration is mainly caused by the lower water vapour transport rate, i.e., lower activity coefficient of water vapour pressure. Furthermore, high concentration of dye increases the attachment of dye particles on the membrane surface, causing a partial or full pore blockage.

Membrane fouling involves pore blockage and aggressive formation of a cake layer, typically induced by the interaction between the membrane, the solutes in solution and operating conditions. Fouling takes place through various mechanisms, typically (a) complete blocking, (b) standard blocking, (c) intermediate blocking, and (d) cake filtration (Fig. 5a) (Yang et al., 2022a). In compete blocking, the solutes seal all the membrane pores. In standard blocking, the solutes are adsorbed or deposited within the membrane pores (Hairom et al., 2014). The continuous accumulation of the particles within the membrane pores increases the size of the foulant, ultimately causing complete pore clogging. In intermediate blocking, the particles form an accumulative layer on the surface of the membrane. Meanwhile, the combination of this layer, presence of coordinating metals and CP establishes a cake layer, resulting in cake filtration (Zhang and Ding, 2015). Membrane

Table 1
Applications of MD process for the removal of dyes from textile effluent.

Membrane materials	MD configuration	[a]Operating Parameter	Dye/concentration	[b]Flux	Ref
High-impact polystyrene (HIPS) and styrene-acrylonitrile (SAN4)	DCMD	$T_f = 52 \pm 2$ °C $T_p = 12 \pm 3$ °C $Q_f = 0.24$ L min^{-1} $Q_p = 0.48$ L min^{-1}	2000 mg L^{-1} reactive orange-122 2000 mg L^{-1} disperse red-60	Reactive Orange-122 $J_i = 38.77$ kg m^{-2}·h^{-1} $J_f = 35.29$ kg m^{-2}·h^{-1} T = 6 h Disperse Red-60 $J_i = 36.33$ kg m^{-2}·h^{-1} $J_f = 23.40$ kg m^{-2}·h^{-1} T = 6 h	Roberto et al. (2020)
Polytetrafluoroethylene (PTFE)	DCMD	$T_f = 60$ °C $T_p = 20$ °C	400 mg L^{-1} reactive blue	Reactive blue dye $J_i = 3.33$ kg m^{-2}·h^{-1} $J_f = 3.40$ kg m^{-2}·h^{-1} T = 7 h	(Criscuoli et al., 2008a), (Ahmad et al., 2018)
Polyetherimide (PEI) membranes and modified by polydimethylsiloxane (PDMS)	SGMD	$T_f = 60$ °C $T_p = 20$ °C $Q_f = 0.20$ L min^{-1} $Q_p = 0.10$ L min^{-1}	1000 mg L^{-1} methylene blue	Methylene blue (pristine PEI) $J_i = 24.17$ kg m^{-2}·h^{-1} $J_f = 13.96$ kg m^{-2}·h^{-1} T = 130 h Methylene blue (PEI with PDMS) $J_i = 21.88$ kg m^{-2}·h^{-1} $J_f = 17.71$ kg m^{-2}·h^{-1} T = 130 h	Criscuoli et al. (2008a)
Poly(tetrafluoroethylene) (PTFE)	DCMD	$T_f = 60$ °C $T_p = 20$ °C $Q_f = 1.5$ L min^{-1} $Q_p = 0.5$ L min^{-1}	1000 mg L^{-1} reactive black 1000 mg L^{-1} disperse black	Reactive black $J_i = 14.46$ kg m^{-2}·h^{-1} $J_f = 10.89$ kg m^{-2}·h^{-1} T = 4 h Disperse black $J_i = 11.43$ kg m^{-2}·h^{-1} $J_f = 6.52$ kg m^{-2}·h^{-1} T = 4 h	Raman and Kanmani, 2016), (Jain et al., 2021)
Poly(tetrafluoroethylene) (PTFE) with polypropylene (PP) support layer	DCMD	$T_f = 60$ °C $T_p = 20$ °C $Q_f = 0.5$ L min^{-1} $Q_p = 0.5$ L min^{-1}	100 mg L^{-1} congo red	Congo red $J_i = 28.10$ kg m^{-2}·h^{-1} $J_f = 14.20$ kg m^{-2}·h^{-1} T = 24 h	Raman and Kanmani (2016)
Polyvinylidene fluoride (PVDF)	DCMD	$T_f = 70$ °C $T_p = 20$ °C	7 mg L^{-1} maxilon blue 5G 7 mg L^{-1} drimarene yellow K-2R 7 mg L^{-1} sodium fluorescein	Maxilon blue 5G $J_i = 21.80$ kg m^{-2}·h^{-1} $J_f = 18.62$ kg m^{-2}·h^{-1} T = 47 h Drimarene yellow K-2R $J_i = 21.20$ kg m^{-2}·h^{-1} $J_f = 20.04$ kg m^{-2}·h^{-1} T = 47 h Sodium fluorescein $J_i = 21.70$ kg m^{-2}·h^{-1} $J_f = 19.35$ kg m^{-2}·h^{-1} T = 47 h	Al-Tohamy et al. (2022)
Poly(tetrafluoroethylene) (PTFE)	AGMD	$T_f = 60$ °C $T_p = 20$ °C $Q_f = 0.38$ L min^{-1} $Q_p = 0.60$ L min^{-1}	100 mg L^{-1} textile wastewater mixtures of sodium chloride with sunset yellow 100 mg L^{-1} rose bengal	Sodium chloride with sunset yellow $J_i = 12.36$ kg m^{-2}·h^{-1} $J_f = 12.00$ kg m^{-2}·h^{-1}	An et al. (2017)

(*continued on next page*)

Table 1 (*continued*)

Membrane materials	MD configuration	[a]Operating Parameter	Dye/concentration	[b]Flux	Ref
				T = 20 h Sodium chloride with rose Bengal $J_i = 10.27$ kg $m^{-2}·h^{-1}$ $J_f = 9.82$ kg $m^{-2}·h^{-1}$ T = 20 h	
Poly(tetrafluoroethylene) (PTFE)	DCMD	$T_f = 60$ °C $T_p = 20$ °C $Q_f = 1.5$ L min^{-1} $Q_p = 0.5$ L min^{-1}	30 mg L^{-1} reactive black 30 mg L^{-1} disperse black	Reactive black $J_i = 18.55$ kg $m^{-2}·h^{-1}$ $J_f = 13.68$ kg $m^{-2}·h^{-1}$ T = 24 h Disperse black $J_i = 22.37$ kg $m^{-2}·h^{-1}$ $J_f = 18.42$ kg $m^{-2}·h^{-1}$ T = 24 h	Shirazi et al. (2014)
Poly(tetrafluoroethylene) (PTFE) with polypropylene (PP) support layer	DCMD	$T_f = 60$ °C $T_p = 20$ °C $Q_f = 0.5$ L min^{-1} $Q_p = 0.5$ L min^{-1}	500 mg L^{-1} congo red	Congo red $J_i = 34.23$ kg $m^{-2}·h^{-1}$ $J_f = 12.50$ kg $m^{-2}·h^{-1}$ T = 24 h	Yang et al. (2021)
PVDF-co-hexafluoropropylene (PVDF-co-HFP)	DCMD	$T_f = 50$ °C $T_p = 7$ °C $Q_f = 1.8$ L min^{-1} $Q_p = 1.8$ L min^{-1}	100 mg L^{-1} methylene blue (MB) 100 mg L^{-1} congo red + 4% NaCl	Methylene blue, congo red and NaCl $J_i = 5.10$ kg $m^{-2}·h^{-1}$ $J_f = 3.40$ kg $m^{-2}·h^{-1}$ T = 6 h	Mokhtara et al. (2016)

[a] Feed temperature: T_f, Feed flowrate: Q_f, Permeate temperature: T_p. Feed permeate: Q_p.
[b] Initial flux: J_i, Final flux: J_f, Sampling time: T.

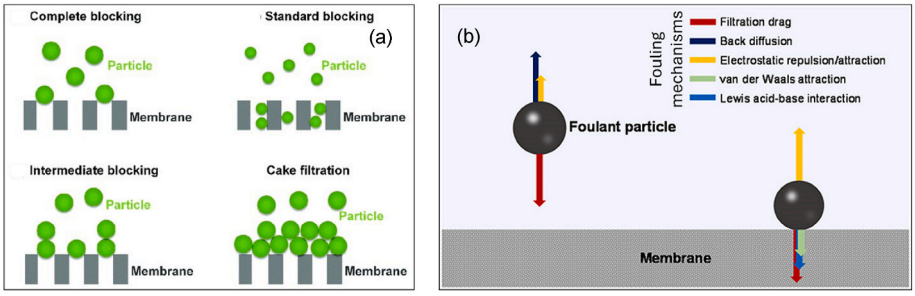

Fig. 5. Schematic illustration of (a) pore blocking causing mass transfer resistance and (b) membrane fouling mechanisms (Yang et al., 2022a; Xu et al., 2020).

fouling of MD processes is a complex phenomenon requiring an understanding of the parameters affecting it to establish its mechanisms. Fouling is affected by various factors namely, (a) membrane properties including hydrophobicity, pore size, roughness, surface charge, functional groups, (b) feed water chemistry including solubility, diffusivity, hydrophobicity, pH, ion strength, type of foulant, and (c) operating conditions such as flow velocity, processing temperature, and transmembrane pressure (TMP).

The identity of the membrane fouling is dependent on feed water, foulant characteristics, and different membrane properties. Typically, hydrophobic membranes foul more compared to hydrophilic membranes. Also, membrane roughness causes excessive fouling due to air entrapment which promotes the fluid drop on the surface of the membrane. According to DLVO theory, the membrane-foulant and foulant-foulant interactions are described by the van der Waal, electrical and acid-base interactions (Fig. 5b) (Yang et al., 2022a). Briefly, the foulants of opposite charges will interact electrostatically. The electrostatic interaction can be attractive or repulsive depending on the direction of the membrane-foulant charges. Also, depending on the membrane and foulant properties, hydrophobic-hydrophobic interactions occur, which is often difficult to break. Submerging of the membrane in water disturb the hydrogen bonds of the molecule, which in turn increase the membrane surface free energy. Upon interaction with the foulant, the high surface energy promotes fouling. In the presence of metal ions, the covalent interaction takes place through metal-organic complexation (Xu et al., 2020). For instance, the multivalent ions such as calcium form bridged complexes between the membrane surface and carboxylic groups present on the foulant.

Since the pressure difference across the membrane during MD process is minimal, the formation of the cake layer due to dye deposition is significantly slower compared to the pressure-driven membrane processes such as NF and reverse osmosis (RO) (Mahlangu et al., 2023a; Ahmed et al., 2023). Ramlow et al. (2020) evaluated the performance of PTFE membrane for textile wastewater treatment using DCMD process (Ramlow et al., 2020). Reportedly, the membrane performance declined moderately from 28.68 to 19.47 kg $m^{-2}·h^{-1}$ over the sampling time due to the accumulation of foulants on the membrane surface. Although the deposited dyes could be effectively removed from the membrane via

physical and/or chemical cleaning, the presence of surfactants in the wastewater react chemically with the dyes, making flux recovery process difficult. Using PTFE membrane for textile wastewater treatment via DCMD process, Fortunato et al. (2021) reported a strong inverse correlation between the membrane fouling layer and the normalized membrane vapour flux (Fortunato et al., 2021). The authors attributed this phenomenon to the cake-enhanced temperature polarization (CETP). As the feed temperature increased, the flux was decreased due to the increased foulant deposition. Therefore, MD operation with low feed temperatures (40–60 °C) is imperative to minimize membrane surface fouling. The hydrophobic nature of textile and cosmetic industry dyes increases the rate of their adsorption on the hydrophobic membrane.

Dye molecules adsorb onto the membrane surface due to attractive forces such as van der Waals, hydrogen bonding, and electrostatic interactions. Once adsorbed, the dyes form a blocking layer on the pores and hinders water flow (Haleem et al., 2023). Adsorption of dye onto the membrane surface is influenced by process conditions (e.g., dye concentration, solution pH, solution temperature, and contact time) and membrane characteristics (e.g., degree of hydrophobicity, pore size distribution, porosity, and charge) (Yang et al., 2022b). Among other factors, pH plays an important role in adsorption, with high affinity of cationic dyes due to their negative surface charges, while anionic dyes with positive surface charges present high affinity to membrane surfaces. Cationic dye adsorption is favoured at pH values greater pH point of zero charge (pH_{pzc}), whereas anionic dye adsorption is favoured at pH values lower than pH_{pzc} (Aijaz et al., 2023).

Additionally, the dye concentration affects the adsorption capacity onto the membrane. At the early stage of dye attachment, adsorption rate increases with the increase in dye concentration. Upon saturation, the adsorption rate decreases due to the repulsion between the adsorbed dye molecules. On the other hand, the adsorption capacity increases at high temperatures following the increase in the mobility of dye molecules (shekhi Abadi et al., 2023). Similarly, the membrane pore size influence the dye adsorption efficiency, with dye molecules absorbing into large pore size (Chidambaram et al., 2015). The typical pore sizes of MD membranes suitable for dye removal range from 0.2 to 1.0 μ m (Camacho et al., 2013; Reddy et al., 2022). In addition to pore size, liquid entry pressure of membranes should be 1.2, 3.1 and 3.6 bar for PP, PVDF, and PTFE membrane, respectively to prevent the penetration of liquid into membrane pores in textile wastewater treatment (Silva et al., 2021a).

Some common dyes react chemically with the membrane through the formation of single or multi-chelates, creating complexes, and oxidation-reduction-absorbance reactions (Hidalgo et al., 2020). Furthermore, the membrane pores accelerate interactions between the dye molecules and the membrane through hydrogen bonding, thus contributing to dye adsorption. The dye molecules, with sulfonic groups and aromatic rings, exhibit strong electrostatic interactions and π-π stacking with the spongy materials. Hydrogen bonding further reinforces this interaction (Hairom et al., 2014). Table 2 presents the mechanism of fouling comparing different types of dyes described in the recent literature.

Table 2
Types of dye vs. mechanism of interactions with the membranes during MD processes.

Membrane type	Dye	Classification of dye	Mechanism	Ref.
DCMD	Congo red	azo dye/ anionic	hydrophobic interactions between the surface of the membrane and dye molecules	Khumalo et al. (2019)
MD	Methylene blue	azo dye/ cationic	electrostatic interaction (EI) and π-π conjugation	Hou et al. (2020)
VMD	Methylene blue	azo dye/ cationic	surface adsorption	Parakala et al. (2019)
DCMD	Acid Red 18	azo dye/ anodic		Benkhaya et al. (2023)
MD	Direct Blue 6	azo dye/ cationic		Benkhaya et al. (2023)
MD	Malachite green	azo dye/ cationic	surface adsorption	Elwardany et al. (2023)
DCMD	Methylene blue	azo dye/ cationic	not specified	Elgharbi et al. (2024)
MD	Direct blue 53 and Acid black 1	azo dye/ anionic	electrostatic interactions, surface adsorption	Chidambaram et al. (2015)
MD	Acid red 87, Azure A, Basic blue	azo dye/ cationic	electrostatic interactions, surface adsorption	Chidambaram et al. (2015)
DCMD	methylene blue, crystal violet13	azo dye/ cationic	electrostatic interactions, surface adsorption	An et al. (2016)
DCMD	acid red 18, and acid yellow 36	azo dye/ anionic	electrostatic interactions, surface adsorption	An et al. (2016)
MD	reactive yellow, reactive red, reactive blue, and reactive black	reactive dyes	electrostatic interactions, van der Waals forces, dye aggregates formation onto membrane surface	Ramlow et al. (2019b)
MD	disperse yellow, disperse red, disperse blue, and disperse black	disperse dyes	electrostatic interactions, van der Waals forces, dye aggregates formation onto membrane surface	Ramlow et al. (2019b)

3.1. Effects of fouling on process performance

The presence of the dye molecules on the membrane surface or within pores adversely affect the membrane hydrophobicity and its antiwetting properties. Previous study analysed the fouling conditions caused by dye molecules via optical coherence tomography (OCT) scanning (Fig. 6a) (Fortunato et al., 2021). According to the reported findings, the perpendicular feed flow increased the thickness of fouling layers along the membrane length (Fig. 6b). Fouling form a resistant layer on the membrane surface, promoting a mass transfer resistance (Laqbaqbi et al., 2019b). Persistent development of fouling layer cause excessive flux decline, with an ultimate degradation of the MD process performance (Mokhtar et al., 2016). Fig. 6c presents the cross-sectional structure and the inner surface field emission electron scanning microscope (FESEM) images of the fouled membrane after a 40-h treatment of industrial textile wastewater (Mokhtar et al., 2016). The inner structure of membrane was severely covered by dye particles altering its surface characteristics and causing remarkable flux decline (Fig. 6d).

According to Fortunato et al. (2021), flux decline is directly related to the fouling layer on the membrane (R^2: ~0.96) (Fortunato et al., 2021). Although the process can be increased by operating at higher feed temperatures, such approach is associated with several negative challenges, degrading both the membrane and the flux. Exposing the membrane to high temperatures for extended periods reduce their lifespan due to material damage. The high thermal stress cause changes in the membrane material, such as loss of hydrophobicity, changes in pore size and structural damage, ultimately decreasing the membrane's efficiency and performance. Additionally, at high operating temperatures,

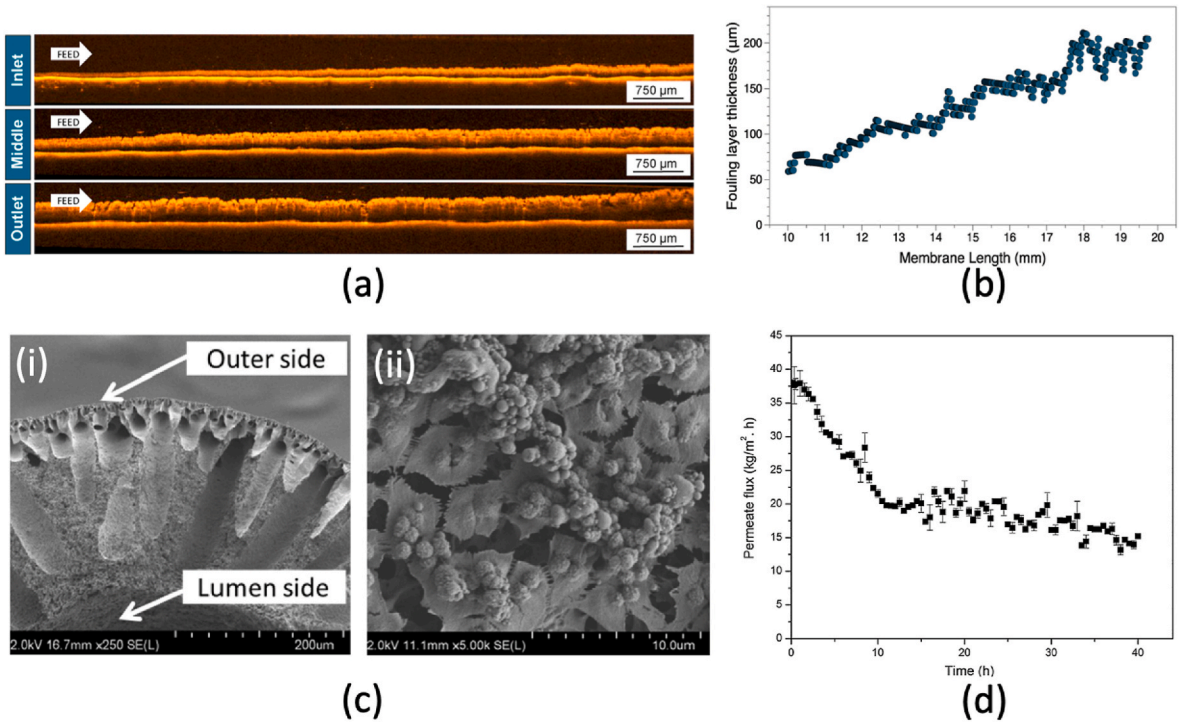

Fig. 6. (a) OCT scan of fouling characteristics at inlet, middle and outlet positions on the membrane surface after 24-h sampling time (feed flow at perpendicular direction) via MD process and (b) Thickness of fouling layer along the membrane length (Testing conditions: temperatures of feed and permeate at 60 °C and 20 °C, respectively, cross-flow velocities of feed and permeate stream at 0.14 m s^{-1} (Fortunato et al., 2021). (c) FESEM images of Cloisite 15A-modified PVDF hollow fibre membrane used for industrial textile wastewater treatment, (i) Partial view of the membrane structure and (ii) accumulation of dye molecules in the inner surface of the membrane and (d) permeate flux as a function of time (Testing conditions: feed and permeate temperatures at 90 °C and 25 °C, respectively, feed and permeate cross-flow velocities of at 0.023 m s^{-1} and 0.002 m s^{-1}, respectively and hot feed solution flowing through membrane lumen) (Mokhtara et al., 2016).

the CP is more pronounced. It occurs when solutes in the feed solution accumulate near the membrane surface, creating a concentration gradient and hindrance of water vapour transport (Tai et al., 2023). Additionally, high operating temperature difference increases energy consumption, thus making MD process costly compared to the pressure-driven membrane processes.

In addition to flux decline, fouling induce physical damage of the membrane (Charfi et al., 2021). These include changes in pore structure, size distribution and decreased mechanical strength (Alsawaftah et al., 2021). Consequently, membrane resistance to wetting is reduced, thus compromising dye separation efficiency and distillate quality (Alkhatib et al., 2021). Mousavi et al. (2021) reported a decrease in methylene blue rejection for both the PEI and PEI-PDMS membranes during 120-h MD experiment (Mousavi et al., 2021b). Reduced dye rejection was associated with membrane pore wetting.

Also, fouling affects the overall economic cost of MD treatment plants, and therefore requires a critical attention. To restore process efficiency after fouling, periodic cleaning is carried out, thus increasing the process operational costs. According to Adel et al. (2022), membrane cleaning should be conducted immediately when the flux drops below 10% to prevent irreversible fouling (Adel et al., 2022). Nevertheless, frequent cleaning (particularly involving chemical agents) promotes downtime and affect membrane structure which ultimately impact the overall operating cost.

3.2. Fouling control strategies

3.2.1. Membrane materials development

The development of advanced membrane materials has been extensively explored as an effective strategy to reduce fouling in MD dye treatment processes. The accumulation of dye molecules and other foulants on the membrane surface hinders the MD process, reducing membrane flux, and compromising separation efficiency (Lim and Ooi, 2022). Hydrophilic coatings, such as SAN, PVA, polyethylene glycol (PEG), CNTs, and silver nanoparticles (AgNPs) have been previously used to modify membrane surface to increase their surface hydrophilicity (Li et al., 2022; Nthunya et al., 2019c, 2020; Mpala et al., 2023a). Hydrophilic coatings play a significant role in reducing dye fouling in MD. It creates a strong affinity for water molecules, establishing a repelling barrier. This reduces the attachment of dye molecules on the membrane, thus minimizing fouling. Additionally, the coatings promote self-cleaning of the membrane surface. When water vapour condenses on the hydrophilic surface, it forms a thin water film capable of detaching the foulants from the membrane. Zwitterionic polymers, characterized by positive and negative charges demonstrated excellent anti-fouling properties (Maity et al., 2022). When grafted onto the membrane surface, these polymers create a repulsive force against dye molecules and foulants, preventing their attachment to the membrane (Maity et al., 2022). Fig. 7a illustrates the improved surface properties of PVDF membrane in reducing the affinity of dye molecules and foulants on the membrane surface, aiming to mitigate fouling and improve flux (Huang et al., 2023). Huang et al. (2023) deposited multiple layers of sulfobetaine methacrylate (SBMA) and acrylic acid (AA) on a hydrophobic PVDF membrane using the layer by layer (LbL) polyelectrolyte deposition technique to produce the wetting and fouling-resistant membrane (Huang et al., 2023). Although coating improved membrane resistance to flux decay, it reduced the membrane pore sizes, thus minimizing the initial permeate flux of the process (Fig. 7b). Shirazi et al. (2020) developed a dual-layer, hydrophobic/hydrophilic SAN4-HIPS membrane embedded with microspheres through a gas-assisted electrospinning technique (Shirazi et al., 2020b). This novel nanofibrous membrane was evaluated for its efficiency in treating hot dyeing effluent using DCMD (Shirazi et al., 2020b). The membrane exhibited desirable properties, such as high permeate flux of 28.31 kg

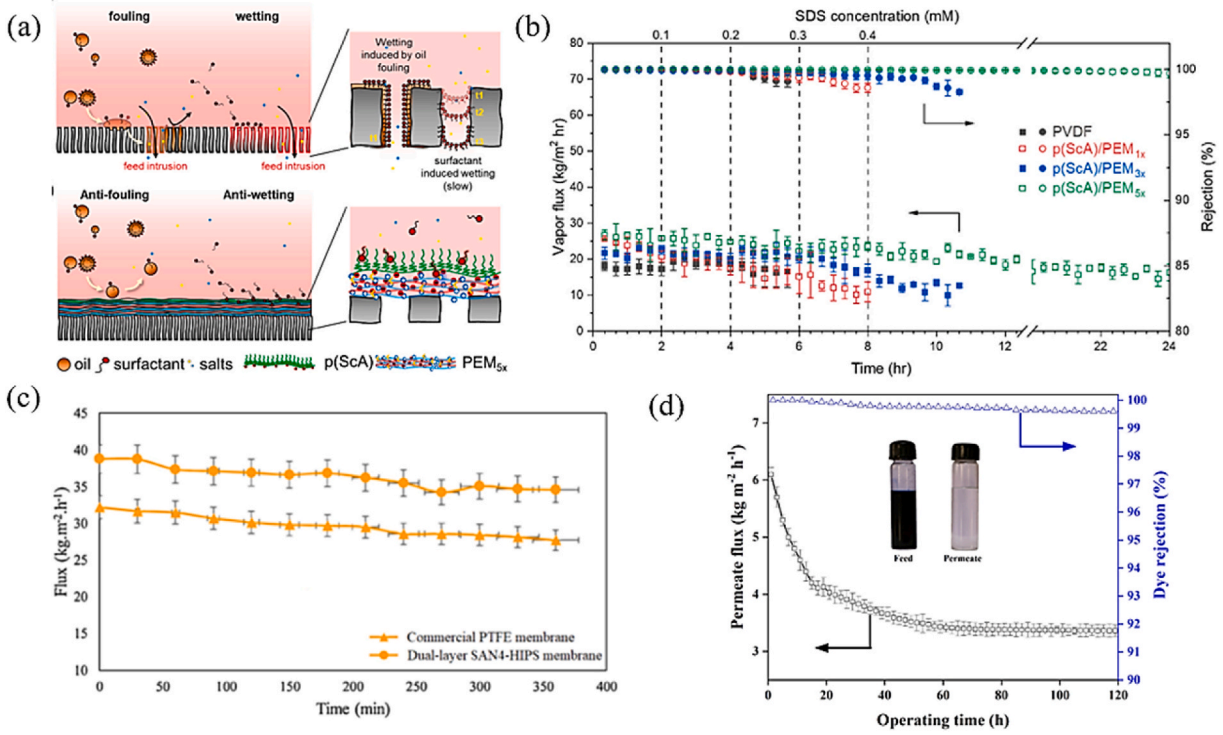

Fig. 7. (a) Fouling of the pristine and hydrophilic-coated membrane (Huang et al., 2023) and (b) Permeate flux and rejection of the hydrophilic-coated membrane during MD process (feed solution: 3.5 wt% NaCl) (Huang et al., 2023). (c) Permeate flux of dual-layer SAN4-HIPS membrane and commercial PTFE membrane during treatment of reactive orange-122 dye wastewater using DCMD (Testing conditions: temperatures difference of feed and permeate: 53 °C, feed and permeate flowrate were set at 0.48 L min^{-1} and 0.24 L min^{-1}, respectively and hot feed solution flowing through membrane lumen) (Shirazi et al., 2020b). (d) Permeate flux and dye rejection of 3 wt% TiO_2-modified PVDF-co-HFP matrix membrane during DCMD process (Yadav et al., 2021b). (For interpretation of the references to colour in this figure legend, the reader is referred to the Web version of this article.)

$m^{-2}.h^{-1}$ with a 99% dye rejection. Also, the membrane presented excellent resistance to pore wetting throughout 50-h dye wastewater treatment (Fig. 7c). Photocatalytic nanoparticles embedded onto the membrane degrade dye molecules under UV irradiation (Liu et al., 2021). This self-healing mechanism helps to maintain a clean membrane surface and reduce fouling. Yadav et al. (2021) successfully fabricated membranes with UV-cleaning properties by integrating porous titanium dioxide (TiO_2) into the PVDF-co-HFP membrane (Yadav et al., 2021b). The TiO_2 NPs were synthesized using controllable large-scale synthesis protocols involving spray drying followed by calcination. In this study, a membrane incorporating 3 wt% TiO_2 NPs demonstrated ~100% dye removal efficiency for MB and CR. Although the membrane flux was reduced as a function of time, a stable flux was attained during the first 50-h operation (Fig. 7d). Furthermore, the DCMD experiments presented a remarkable 91% flux recovery rate after 4-h UV-cleaning.

3.2.2. Process control

The MD operates based on thermal principles, with its flux performance relying heavily on water vapour transfer across the membrane. However, accumulation of scalants and foulants on the membrane surface decreases the vapour pressure, resulting in a permeate flux decline. Thus, effective control of operating parameters, especially vapour pressure and feed temperatures are crucial in maintaining optimal flux output in the presence of foulants (Choudhury et al., 2019). The Antoine equation **(Equation (1))** governs the relationship between the vapour pressure and the feed temperature. This equation describes the heat and mass transfer phenomena in MD process. The high vapour pressure and the permeate flux are attained at high feed temperatures. Besides improving permeate flux (Choudhury et al., 2019), elevated feed temperatures reduce TP, leading to enhanced mass transfer across the membrane (Silva et al., 2021b). Criscuoli et al. (2008) conducted an experimental study to remove Remazol Brilliant Blue R dye using VMD process. The results presented a two-fold increase in flux from 27.5 to 57 kg $m^{-2}.h^{-1}$ upon increase in feed temperature from 40 °C to 60 °C (Criscuoli et al., 2008b).

$$\log_{10}(p) = A - \frac{B}{C + T} \quad [1]$$

where p is the absolute vapour pressure, T is the temperature (in degree Celsius) and A, B, and C are Antoine coefficients specific to the substance.

Besides optimizing the feed temperature alone, Hickenbottom and Cath (2014) investigated temperature and flow reversal techniques as novel approaches to effectively mitigate fouling in MD process and restore flux and salt rejection (Yan et al., 2021). In the flow reversal method, the feed side and the permeate side channels were reversed (i.e., the feed side becoming the permeate side and vice versa). The temperature reversal method utilizes a cyclic process where a cold feed stream is circulated without heating, while the temperature on the distillate side of the membrane is maintained. After a specific sampling time, the hot feed stream is circulated into the distillate side of the membrane, effectively reversing the driving force across the membrane. Prior to either flow or temperature reversal implementation, the DCMD evaluation was stopped before scaling occurred or after recovering 35–40% of the feed water. The results indicated the successful maintenance of water flux and salt rejection using both methods, with the temperature reversal method exhibiting better overall performance (Yan et al., 2021). Both techniques effectively inhibited homogeneous salt precipitation and disrupted the nucleation of salt crystals on the membrane surface, leading to reduced fouling and improved membrane performance.

To prevent dye fouling in MD, the AGMD, SGMD, and VMD are commonly considered advantageous. In AGMD, there is an air gap

between the membrane and the condensation surface. The feed solution is circulated on one side of the membrane, and cold air or an inert gas is passed on the other side to condense the vapour. The air gap acts as a physical barrier, preventing direct contact between the membrane and the condensation surface, thus reducing fouling. In this case, dye molecules are less likely to come in direct contact with the membrane surface, thereby minimizing fouling (Hitsov et al., 2018). The SGMD involves the use of a continuous flow of a sweeping gas (e.g., air or nitrogen) on the permeate side of the membrane. The sweeping gas carries away the vapour molecules that pass through the membrane, preventing them from condensing on the permeate side and reducing the CP. This setup helps to maintain a clean and clear permeate side, minimizing the chances of dye molecules accumulation on the membrane surface (Qin et al., 2018). The VMD is characterized by low-temperature differences due to negligible heat conduction, thus minimizing polarization and reduces fouling. However, the VMD is susceptible to wetting due to possible operating pressure exceeding the membrane LEP, thus compromising the separation efficiency.

3.2.3. Cleaning processes

Exploring the factors influencing membrane fouling is crucial to decrease the fouling rate and prolonging the membrane lifespan in the MD process. Nonetheless, it is practically impossible to avoid fouling in the membrane processes. Thus, cleaning becomes important to remove foulants from the membranes. According to the reported findings, membrane cleaning mechanism is mainly categorised into pre-treatment, physical and chemical cleaning with the latter being more effective to remove the foulants and scalants deposited on the membrane (Adel et al., 2022). Dow et al. (2017) evaluated effectiveness of foam fractionation as a pre-treatment method for textile effluent prior MD purification (Dow et al., 2017). To produce the "fractionated MD feed," the textile effluent was treated through a foam fractionation. Afterwards, the pretreated feed was directed into the MD process for further treatment. Foam fractionation aims to remove surface-active agents, especially dye molecules from the feed stream by injecting it with compressed air. During foam fractionation, the feed water flowed down a column with an exposure to rising finely dispersed air bubbles. The gas bubbles effectively captured surface-active materials, lifting them to the top of the water column to form a foam layer. This foam layer was subsequently collected in a foam trap and removed from the system. According to the reported findings, the flux of the membrane module (effective surface area: 6.4 m^2) was only reduced from an initial rate of 5 to 2 L $m^{-2}{\cdot}h^{-1}$ after more than 1560-h of continuous operation without having membrane cleaning process.

In practice, chemical cleaning restores the membrane's initial performance to certain degree depending on the severity of fouling (Fig. 8). Manzoor et al. (2022) investigated the impact of chemical cleaning using 2 wt% sodium hypochlorite (NaOCl) and 2 wt% citric acid in a novel hybrid MD combined with a submerged anaerobic membrane bioreactor to remove cibacron yellow, cibacron blue and methylene blue dyes (Manzoor et al., 2022). The chemical cleaning procedure was implemented when the flux dropped to approximately 80% of the initial flux. To ensure optimal flux recovery, the module was detached from the MD system. The membrane was first washed with tap water to eliminate sludge layers and other impurities accumulated on its surface. Subsequently, chemical cleaning was carried out, involving a 15-min soaking of the membranes in NaOCl solution to remove organic foulants. This was followed by exposure to citric acid solution to remove inorganic foulants. The chemical cleaning approach achieved 84.8% flux recovery (Fig. 8a).

According to Shi et al. (2022), a combined chemical cleaning approach, involving the use of absolute ethanol and 0.1 mol L^{-1} NaOH effectively maintain the permeate flux of VMD during purification of CR dye (Shi et al., 2022). The hollow fibre membrane demonstrated a remarkable dye rejection ≥99%. However, the permeate flux gradually decreased from 18.2 [1]–9.6 kg $m^{-2}{\cdot}h^{-1}$ after 8-h operation. To minimize flux decline, a cleaning solution comprised of absolute ethanol and NaOH was introduced as the feed solution and circulated through the fibre lumen using a diaphragm pump under 0.1 MPa for 1 h. Subsequently, the membrane was further washed with pure water for 30 min. The cleaning process gave rise to a remarkable 90% permeate flux recovery (Fig. 8b).

To the best of our knowledge, physical cleaning methods are not widely studied in MD for dye removal. This is mainly attributed to the nature of dye fouling in MD, which often involves the adsorption and deposition of dye molecules on the membrane surface. These foulants exhibit a strong affinity to the membrane material, leading to robust adhesion. As a result, physical cleaning methods are not effective in removal of dye solutes from the membrane. Moreover, membranes used in MD process typically have a small pore, making it challenging to physically access and clean dye foulants from the membrane microstructure. Julian et al. (2018) evaluated air backwashing to restore the flux of VMD membrane during desalination of the brine (Julian et al., 2018). According to the research findings, magnesium deposition on the surface and pores of the membrane, reducing flux upon increase in frequency and duration of backwashing. Magnesium disposition was induced by nucleation causing salt crystallization. To some extent, air backwashing reduced the membrane scaling. However, other physical methods such as aeration and Vibration/ultrasound presented improved flux restoration of MD systems (Abdel-Karim et al., 2021). In aeration, the air bubbles promote formation of the shear force which reduce the cake layer formation on the membrane. In vibration processes, the cavitation is formed from small bubbles (Abdel-Karim et al., 2021). The collapse of these cavities generates shockwaves which detach the foulants from the membrane.

3.2.4. Hybrid/integrated MD processes

Treatment of dye wastewater through Integrated chemical and

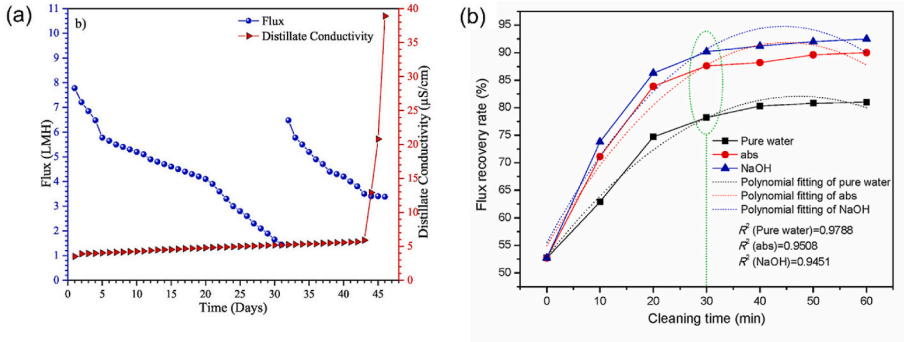

Fig. 8. (a) Permeate flux and conductivity during 2 wt% NaOCl and 2 wt% citric acid chemical cleaning (Manzoor et al., 2022). (b) Comparison of different chemical cleaning methods in retrieving the flux of membrane used for VMD process towards CR dye removal (Shi et al., 2022).

treatment processes has gained a remarkable research attention. Research has been focused on the hybridization of photocatalysis and membrane separation, also known as photocatalytic membrane reactors (PMR) (Su et al., 2016). However, coupling of MD with other membrane systems for the removal of dyes from wastewater has been evaluated extensively (Ibrar et al., 2022; Ge et al., 2012). Ge et al. (2012) used a polyelectrolyte-promoted forward osmosis-membrane distillation (FO-MD) hybrid system to recycle acid dye-containing wastewater (Ge et al., 2012). MD was used to reconcentrate the poly(acrylic acid) sodium (PAA-Na) salt used as the solute in the FO process to dehydrate the wastewater. Based on reported findings, FO-MD hybrid process is more efficient than the individual FO process in concentrating acid orange 8 dye present in the wastewater. As suggested by the authors, integration of FO and MD combines the strength of both processes, including low fouling tendency and the potential use of industrial waste heat (Ge et al., 2012).

The FO-MD hybrid process can potentially achieve zero liquid discharge when treating wastewater from the textile industry and recover valuable dye molecules while producing high-quality water. However, efficient FO and MD membranes are required to reduce fouling and advance this hybrid process (Li et al., 2020a). Li et al. (2020) identified an internal concentration polarization (ICP) effect and membrane fouling using two commercial FO membranes, which make it difficult to equilibrate the water transfer rate to reach good performance (Li et al., 2020a). Also, the authors proposed a hybrid FO-MD system composed of an asymmetric membrane and PTFE membrane in the FO and MD units, respectively (Li et al., 2020a). During the test experiments, the draw solution was diluted in the FO process and was simultaneously regenerated in the MD process. The system was able to treat textile wastewater in continuous and stable operation due to the fouling and ICP resistance of the FO symmetric membrane. Also, the use of the symmetric membrane reduced the energy consumption, and the overall cost of a large-scale RO-MD system.

More recently, a FO-MD hybrid process using a newly developed graphene oxide enhanced FO membrane (GFO) was proposed to treat textile wastewater. Wu et al. (2024) used textile wastewater to evaluate the GFO performance (Wu et al., 2024). The feed matrix presented a significant challenge on membrane performance and stability due to a higher degree of fouling and wetting (Choudhury et al., 2019). The GFO membrane was fabricated through interfacial polymerization process by adding GO into the polyamide. The performance of the hybrid system with GFO membrane was compared to the performance of a commercial FO membrane. According to the reported findings, GFO-based FO-MD process presented improved fouling resistance and stable permeate flux. The hybrid system surpassed the individual FO and MD processes by overcoming the limitations of FO draw solution dilution and MD membrane wetting challenges (Wu et al., 2024).

A MD/photocatalysis hybrid process has been studied to treat dye wastewater due to the ability to retain non-volatile compounds (Nadimi et al., 2024). The quality of the permeate in MD/photocatalysis hybrid process is not affected by the presence of the catalyst at concentrations range of 0.1–0.5 g L^{-1} However, concentrations higher than 0.5 g L^{-1} promote formation of a catalyst cake layer on the membrane surface, thus reducing permeate flux (Nadimi et al., 2024). The catalyst characteristic, including the crystalline phase and particle size plays an important role in controlling fouling of the MD/photocatalysis hybrid process during of dye-polluted wastewater. According to Mozia et al. (2008), P25 (TiO_2 in anatase and rutile phase) showed the best performance due to high purity anatase-phase TiO_2 structure (Mozia et al., 2008).

4. Energy consumption and module design

Thermal energy consumption is a critical factor in economic viability and environmental sustainability of any separation process, including MD. In fact, the high energy consumption of MD has been identified as one of the major limitations of the process and different efforts have been devoted to reducing the required thermal energy of the process. The energy consumption and gain output ratio (GOR) of various MD configurations are presented in Table 3.

The main strategies used to reduce the thermal energy requirements of MD include process optimization and utilization of waste thermal energy in the textile industry, innovative module designs and configurations, and fabrication of new membranes with low-thermal losses. On the process end, several parameters including feed and permeate temperatures, feed and permeate flow rates, and properties of the feed solution affect the thermal energy consumption of the process (Christie et al., 2020; Tewodros et al., 2022).

(a) Effect of feed temperature

Flux in MD is exponentially linked with the temperature of the feed solutions whereas the heat conduction through the membrane is linearly related to the temperature difference between the feed and permeate sides (Nthunya et al., 2024; Ali et al., 2018). Therefore, the thermal efficiency of the process, measured as the ratio of convective heat transport to the total heat transport across the membrane, increases with an increase in feed temperatures. However, for poorly insulated systems, high feed temperatures deteriorate the system performance due to the high losses of heat from the feed stream to the environment. According to Elmarghany et al. (2019), the feed temperature presents the adverse impact on thermal efficiency, primarily attributed to heat dissipation from the membrane cell into the surroundings (Elmarghany et al., 2019). The rise in feed temperature resulted in a greater temperature disparity between the cell and its surroundings, causing a 34% reduction in thermal efficiency. Additionally, the obtained output ratio declined from 0.96 to 0.6, accompanied by a rise in specific energy consumption from 689 to 1037 kWh·m^{-3}.

In the case of DCMD, the system performance is dominantly dependent on the feed temperature and the effect of permeate temperature remains relatively minor. For instance, Song et al. (2007) performed a systematic investigation of the effect of feed and permeate temperatures using a commercial hollow fibre membrane module (Song et al., 2007). Reportedly, the increase in feed temperature from 40 °C to 92 °C led to an exponential increase in permeate flux whereas increasing distillate temperature from 32 °C to 60 °C did not influence the flux notably. Shirazi et al. (2020) utilized the waste thermal heat to generate >60 °C for use in pilot scale MD treatment of textile wastewater (Shirazi et al., 2020a). The experiment was conducted during cold season (environmental temperature of 1–5 °C), thus indicating the possible opportunity to reduce the external energy requirement for treating textile wastewater on a large scale. The unique properties of the membrane improved the process performance where a permeate flux and salt rejection of 28.31 kg m^{-2} h^{-1} and 98.15% were recorded respectively compared to the commercial membrane (flux: 18.50 kg m^{-2} h^{-1} and salt rejection: 97.10%), without considerable pore wetting. Also, it was reportedly indicated that new membrane possessed lower LEP owing to its higher porosity, larger maximum pore size (0.76 μm), and thinner structure (150 μm).

(b) Effect of feed flow rate

Feed flow rate is another important parameter influencing the energy consumption of the MD process (Khayet and Cojocaru, 2012; Khayet et al., 2012). The temperature polarization (TP) (which refers to a discrepancy between the temperature of the bulk feed solution and the temperature at the interface of the membrane) remains a significant challenge hindering the thermal efficiency and mass transfer coefficients of the MD process. The feed flow rate affects the residence time of the solution in the membrane module. The flow rate of the hot feed affects the heat transfer efficiency across the membrane. Higher flow rates induce better mixing of the fluid present at the membrane surface and in

Table 3
The comparison of energy consumption and GOR for various MD configurations.

MD configuration and feed solution	Feed and permeate temp. (°C)	Permeate flux ($kg•m^{-2}•h^{-1}$)	Energy consumption ($kWh·m^{-3}$)	GOR	Ref.
DCMD, 3.0% NaCl	41 and 26	6.0	780	0.86	Makanjuola et al. (2021)
AGMD, seawater	64.0 and 20	3.3	605	0.73	Elhenawy et al. (2023)
AGMD, seawater	70 and 25	13.0	1080	0.43	Alawad and Khalifa (2021)
AGMD, 3.5% NaCl	70 and 25	1.0	105	6.5	Duong et al. (2016)
DCMD, seawater	85 and 20	2.1	200	6.0	Koschikowski et al. (2009)
DCMD, seawater	–	2.5	302	0.9	Banat et al. (2007)
AGMD, seawater	85 and 30	3.4	210	–	Zaragoza et al. (2014)
DCMD	80 and 20	1.9	205	5.8	Koschikowski et al. (2003)

the channel leading to reduced TP. This results in higher driving force (temperature differences) to the vapour transport from the feed to the permeate side. Also, a high flow rate decreases the residence time of the feed solution in the membrane module resulting in a high average temperature over the membrane length (Ali et al., 2016). Moreover, higher feed flow rates delay the membrane fouling. This can be more important in case of textile wastewater treatment, as different types of dyes, chemicals, and inorganic compounds are present in the solution (Ramlow et al., 2017).

Although the positive impact of high flow rate on the energy efficiency of MD process is well documented, it should be noted that beyond a threshold level, further increase in flow rate influences the process performance negatively. According to Duong et al. (2016) running the pilot-scale AGMD process with a high-water circulation rate led to a decrease in thermal efficiency (Duong et al., 2016). When the water circulation rate was increased, the time the coolant and hot feed spent inside the membrane module decreased, causing a reduction in the effectiveness of heat recovery. Technically, the recovery of latent heat from water vapour to the coolant diminished, causing an increase in temperature difference between the evaporator inlet and the condenser outlet. The higher water circulation rate increased temperature difference between the evaporator inlet and the condenser outlet, contributing to a rise in the overall heat input to the system. This increase in total heat input occurred at a faster stride compared to the rate of distillate production when the water circulation rate was elevated. Consequently, the specific thermal energy consumption of the system increased from 65 to 105 $kWh·m^{-3}$ as the water circulation rate was raised from 150 to 350 L h^{-1}. Also, this shift caused the GOR of the system to decrease from 9.5 to 6.0. Similar effects of water circulation rate on thermal efficiency were reported in other studies (Summers et al., 2012; Duong et al., 2015). According to the research findings, water circulation rate had a significant impact on the specific electric energy consumption of the system. This was directly related to the water circulation rate and the hydraulic pressure drop across the membrane module. When the water circulation rate was increased from 150 to 350 L h^{-1}, the hydraulic pressure drop increased from 0.14 bar to 0.45 bar. Despite the increase in distillate production rate, the specific electric energy consumption of the system showed a notable increase from 0.1 to 0.4 $kWh·m^{-3}$.

In MD, water vapour mass transfer through the membrane is essential. When the flow rate is too high, the process performance remains relatively constant due to the shift of mass transport limit from the flow channels to the membrane (Lee et al., 2018; Liu et al., 2022). As a result, thermal efficiency of the process decreases, necessitating higher temperatures and subsequently increasing energy consumption. Flow rates influence the pressure drop across the membrane module. Excessively high flow rates elevate pressure drop, leading to increased pumping energy requirements. Balancing flow rates to minimize pressure drop while maintaining sufficient mass transfer is crucial for optimizing energy consumption. Extremely high flow rates increase the risk of membrane wetting, where the hydrophobic membrane becomes wetted by the liquid feed leading to reduced vapour flux and poor permeate quality (Ali et al., 2019). Technically, the pumping pressure should be maintained below the LEP of the membrane.

(c) Effect of module spacers

To overcome the negative impacts associated with the high flow rate in the MD system, various options have been proposed to alleviate the TP and CP. Among other strategies, spacers are used in flat sheet membrane modules (Martínez-Díez et al., 1998; Chernyshov et al., 2005; Martínez and Rodríguez-Maroto, 2006). The spacers (net-like feed channels) enhance performance of MD systems. These spacers, with various designs and orientations, are reported to reduce thermal polarization effects and improve permeate flux (Chernyshov et al., 2005; Phattaranawik et al., 2003). Their introduction leads to a decrease in the temperature differences across the membrane and effectively increases mass transfer rates. However, the increase in spacer void beyond 60% optimal range negatively impact mass flux (Phattaranawik et al., 2003). Despite some pressure drops caused by spacer channels, their benefits in reducing thermal boundary layers and CP are reported (El et al., 2020; Al-Sharif et al., 2013). Achieving optimal conditions for spacer installation in a DCMD system is crucial for maximizing mass transfer efficiency and minimizing heat transfer effects depending on various parameters.

(d) Effect of module design

In addition to spacers, another strategy capable of decreasing the thermal energy requirement of MD is the design of energy-efficient MD modules. A module fundamentally provides housing to accommodate the membranes. However, a more favorable design revolves around embracing a module configuration to boasts superior hydrodynamic conditions on both shell and lumen sides (Ali et al., 2024). Depending upon the configurations of membrane (flat sheet or hollow fibre) and MD (DCMD, AGMD, VMD, and SGMD), several module designs to improve heat and mass transport of MD process have been proposed (Ali et al., 2015; Teoh et al., 2008; Gao et al., 2019).

Notable flat sheet membranes designs include spiral wound modules, muti effect VMD modules, and "gap" MD modules. The latter category mainly involves the module designs built for the AGMD where a gap between the feed and condensing surface is provided. Traditionally, the gap is filled with a thin film of air giving rise to AGMD. However, recent studies use various materials including water, conductive metals and sand to fill the gap, thus giving rise to material gap membrane distillation (MGMD) (Shahu and Thombre, 2019; Im et al., 2022; Tian et al., 2014; Khalifa, 2020). The inclusion of these materials in the gap improves the heat transport from the condensing surface and therefore, yields high flux and lower specific thermal energy consumption. Similar to the flat sheet membrane modules, innovative module designs have been proposed for hollow fibre MD modules. The main innovative aspect of these modules is the shapes of the fibre where helical, wavy, curly, and spacers knitted fibres have been proposed to improve the thermal efficiency of the MD process (Ali et al., 2015; Yang et al., 2013). Notably, most of these studies considered the desalination application of various MD configurations, while few studies on module design have been specifically developed for MD-based textile wastewater treatment. Nevertheless, most of the investigated scenarios in MD module design can be considered for this application as well, either directly or with

some minor modifications according to the nature of effluent from textile industry.

In addition to the new designs of module housing and fibre shapes, the design of optimum contact length (or effective module length) has also been an important parameter to reduce the thermal energy requirement of MD process. Theoretically, greater contact lengths can be achieved by elongating the membrane (or fibre length in hollow fibre setups). However, practical difficulties involving technology, handling, and installation render the preparation and use of very long modules unfeasible. As an alternative, achieving a substantial contact length involves either connecting numerous modules in a series or increasing the membrane length within each section of a flat sheet membrane. In the context of spiral-wound flat sheet membranes, extending the flow channel length from 1 to 7 m increases the GOR by 3-fold (Winter et al., 2017). Similar findings were reported by Winter et al. (2017) where specific thermal energy consumption of MD was reduced from 296 to 107 kWh·m^{-3} after increasing the channel length from 1.5 m to 5 m (Winter et al., 2017). However, in case of textile wastewater treatment, the spiral wound module is highly susceptible to fouling due to high contamination level of dyeing wastewater and its inorganic content. Separately, Ali et al. (2018) reduced the specific energy consumption of DCMD by over 20% after increasing the channel length (with an effect comparable to elongating the module length) from 1 m to 10 m (Ali et al., 2018). Similar findings were reported in another investigation where channel length elongation from 3.5 m to 10 m reduced the specific energy consumption of AGMD by 46% (Winter et al., 2011).

(e) Effect of membrane properties

Membrane properties play a significant role in dictating the energy consumption of the process. Membrane properties including thickness, porosity, tortuosity, and pore size play a crucial role in influencing permeate flux, heat, and mass transfer coefficients. Thinner membranes offer higher mass transfer and flux. Due to the small thickness, the mass transfer resistance is significantly reduced, ensuring high permeate flux. However, this phenomenon establishes a trade-off between heat and mass transfer. Although thinner membranes enhance heat transfer, they cause performance decline. The increased heat transfer increases TP, thus reducing the vapour pressure gradient and therefore the flux. Balancing these properties is key in membrane design.

Based on previous research findings, energy-efficient membranes should have thicknesses between 20 and 60 μm, pore diameters of 0.3 μm for high LEP, porosity above 75%, and specific mechanical strength (Tewodros et al., 2022). According to theoretical and experimental reports, small membrane thickness reduces the thermal efficiency of materials like PVDF and PTFE. For a heat transfer coefficient of 600 W m^{-2} K, membrane thickness in the range of 150–200 μm is considered optimal to achieve 80% efficiency in a DCMD system (Ullah et al., 2018). Therefore, thicker membranes are high energy efficiency during MD treatment of high saline feed water. However, for low solute concentration range, such as diluted textile effluent, thinner membranes can provide higher permeate flux and energy efficiency (Eykens et al., 2016). The development of multilayer membranes emerges another promising approach to address energy efficiency. In this design, a strategically placed insulating layer is situated as the intermediate layer inside the membrane structure. The presence of an insulating layer serves as a thermal barrier, effectively mitigating the transfer of heat by conduction across the membrane, specifically in the DCMD configurations. Afsari et al. (2023) used this approach to develop a novel nanofibre membrane with enhanced total thermal efficiency (Afsari et al., 2023). The authors focused on the development of a triple-layer membrane featuring a nanofibrous structure for processing high salinity water using DCMD. According to the obtained results, the triple-layer membrane structure reduced the energy consumption by 20% in comparison with the traditional single-layer membrane structure.

5. Heat and mass transfer modelling

Mathematical models and numerical designs have been reported in the literature to simulate the flux of VMD configuration (Baghel et al., 2020). These models could be adapted to other MD configurations, including AGMD and SGMD. These models include one-dimensional (1D), two dimensional, and three dimensional (3D) approaches (Baghel et al., 2020; Lian et al., 2016; Haddadi et al., 2018). The 1D models have been used to determine the role of process variables on the MD performance. However, the models are unable to provide information about the module and membrane geometry, which is critical to scale up the process. The 2D models have been used to analyze the permeation rate and heat and mass transfer effect on the MD process. This type of model has limitations in evaluating the membrane characteristics and composition along with the geometry of the module (Baghel et al., 2020). In contrast, the 3D models provide a detailed visualization of the processes occurring inside of the membrane, including the impact of boundary layers and the polarization effects related to the characteristic of the membrane, such as porosity and tortuosity (Baghel et al., 2020). Various case studies evaluating mathematical models and numerical designs are comprehensively elaborated below.

A 3D computational fluid dynamics (CFD) model was evaluated by Baghel et el. (2020) using COMSOL Multiphysics to model the interfacial temperatures for Naphthol Blue-Black dye from wastewater and predict the flux in VMD (Baghel et al., 2020). The CFD model incorporated the transport equations for momentum, heat, and mass transfer. The heat and mass transfer were coupled at the contacting interfacial boundaries between the feed solution and the membrane surface, and the effect of variables such as flow and temperature. Also, the amount of vacuum and concentration on the permeate flux were analysed (Parakala et al., 2019). Similarly, a theoretical permeate flux was evaluated from the convective heat transfer through the porous membrane. The model combined the Knudsen and Poiseuille flow equations to study the vapour transport through the porous membrane (Baghel et al., 2020; Ma et al., 2022). The model fitted well with experimental data and provided the temperature polarization coefficient (TPC) for the VMD process at different operating parameters. Based on the model, the feed temperature and vacuum degree were the main parameters affecting the permeate flux and minimum specific energy consumption. Also, increasing the feed temperature from 25 °C to 85 °C reduced the TPC from 0.81 to 0.48, which was reflected in a reduced heat transfer resistance and a considerably increase of the permeate flux (Baghel et al., 2020).

Fig. 9a shows the temperature contour and convective heat flux inside the membrane of the VMD module at 85 °C as obtained by the CFD model. According to the reported findings, driving force of the process, represented by the difference in transmembrane vapour that increases exponentially when the feed temperature increases, caused this temperature profile (Baghel et al., 2020). The accumulation of dye on the feed side of the membrane during the transport of water vapour through the membrane, caused a resistance to liquid-mass transfer, and therefore reduced the passage of water vapour. The small pore size and hydrophobic properties of the membrane contributed to the accumulation of the dye on the membrane surface. The CP effect on the feed side of the membrane become significant due to the increased accumulation of dye at the membrane surface. Notably, the performance of the VMD process can be improved by removing the dye from the surface of the membrane with distilled water. After 60 h of running and washing the membrane, a 99.9% removal of dye with a permeate flux of 44.94 kg m^{-2}·h^{-1} was obtained, thus presenting 99% flux recovery.

A 3D CFD model was developed to study the thermal velocity and concentration field of a VMD using PFTE membranes to treat methyl orange dye wastewater. Initially, the optimal operating parameters of VMD, including mass flow rate, vacuum pressure, inlet feed temperature, and dye concentration, were optimized using response surface methodology (RSM) (Yadav et al., 2022). A regression model was

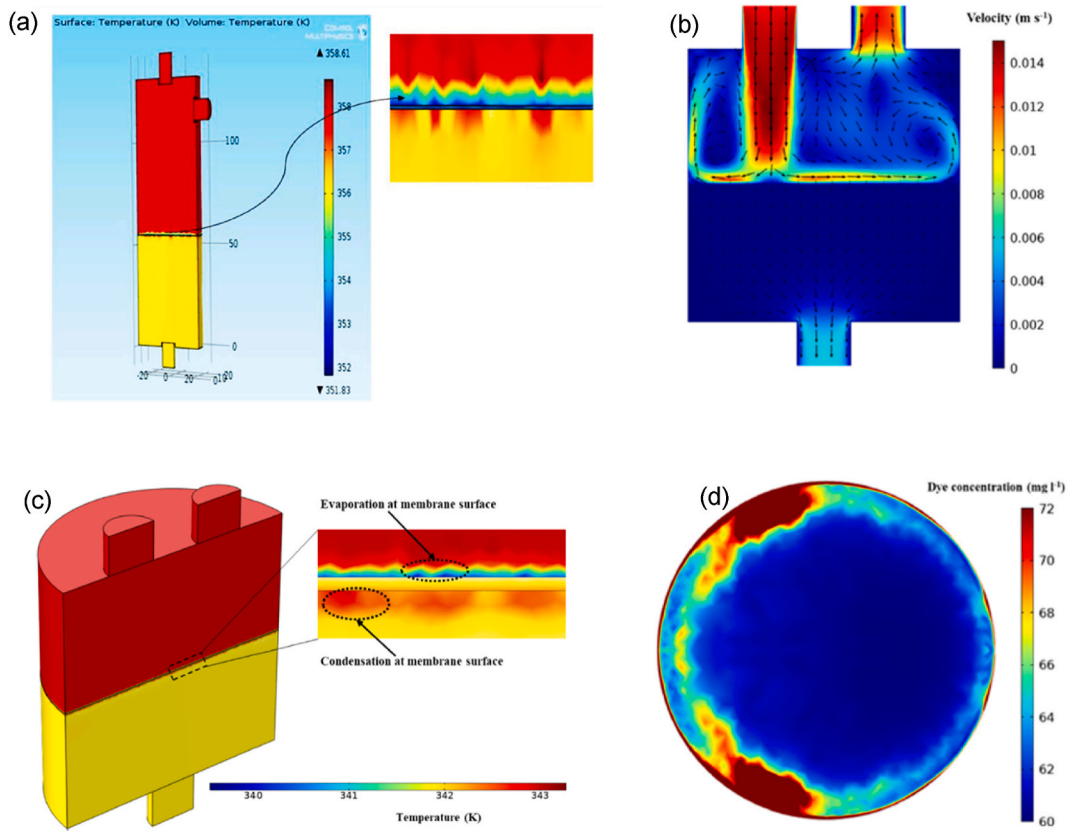

Fig. 9. (a) Temperature contour inside a VMD module at 85 °C feed temperature, Naphthol Blue-Black dye concentration of 300 ppm as simulated by CFD using COMSOL Multiphysics software. Operating conditions: flow rate of 5 L min^{-1}, vacuum of 750 mmHg (Baghel et al., 2020), (b) velocity field, (c) thermal field, and (d) concentration field in the membrane module obtained using 3D CFD at optimized input process parameters from RSM (Yadav et al., 2022). (For interpretation of the references to colour in this figure legend, the reader is referred to the Web version of this article.)

developed to describe the permeate flux, dye rejection, and specific energy consumption (SEC). The 3D CFM model was applied to the optimized parameter conditions (permeate flux of 19.60 L $m^{-2}{\cdot}h^{-1}$, dye rejection of 99.80%, and SEC of 2.04 kWh·m^3) to obtain the permeate flux profile and dye rejection of various cycles of VMD operation with intermittent washing and to understand the fouling behaviour of the membrane. The model captured the evaporation in the feed at the membrane surface and the condensation of vapours in the permeate at the membrane surface. Fig. 9b–d shows the thermal field, velocity field, and concentration field in the membrane module obtained from the 3D CFD of the RSM optimized input process parameters. After conducting SEM analysis of the PTFE membranes, the dye deposition was not severe due to high hydrophobicity, LEP, and pore wetting resistance of the membrane. The membranes exposed to long-term VMD operation didn't show any significant alterations, showing that the PTFE membrane could retain the initial structure and property during dye treatment (Yadav et al., 2022).

A mathematical model incorporating temperature and CP effects was developed by Banat et al. (2005) to treat MB dye solutions generated by the textile industry using VMD (Banat et al., 2005b). The model was validated with experimental data. The model incorporated heat and mass transfer principles, including 1) flux in the boundary layer to the membrane surface, 2) evaporation at the pore entrance and diffusion of the vapour through the pore, and 3) diffusion of the vapour beyond the pore and recovery. The model was validated by comparing the predicted variation of MB concentration with time to the experimental data. The experimental data was comparable with the model predictions. The permeate flux rate decreased exponentially with time, and the dye was concentrated in the feed reservoir without detection in the permeate. The permeate flux was strongly dependent on feed temperature but was independent of salt concentration (Banat et al., 2005b).

As the filtration effectiveness depends on the membrane characteristics, recent studies show the potential of surface modification with carbon-based materials like GO and CNT. GO as 2D material can enhance the operation yield and protect against fouling for its negative charge onto a surface behaving as polyanion. Hence, GO can interact electrostatically with positively charged molecules and materials present in the wastewater enabling electrostatic repulsion of negatively charged molecules like anionic dyes (Hu and Mi, 2014; Homem et al., 2019). Besides 2D materials like GO, other types of nanomaterials that are based on carbon are 1D CNT including single (SWCNT) and multi-walled nanotubes (MWCNT). They are added to reduce the wettability of the membrane for their hydrophobic properties (Mpala et al., 2023b). Moreover, their high surface area and porosity improves absorption of the pollutants in selected wastewater treatment applications. Membranes modified with CNT offer enhanced mechanical stability, self-cleaning functions, and anti-fouling capacity of the nanocomposite membrane (Ray et al., 2020). The immobility of the CNT into the membrane surface occurs due to charge, van der Waals interactions, and chemical bonding (Petukhov and Johnson, 2024).

To improve the hydrophobicity of the membranes, the ZIF NPs can also be added. Tournis et al. (2022) proposed the use of ZIF NPs to modify the porous PVDF–HFP membranes. Membrane modification significantly reduced the wettability of the membrane (Tournis et al., 2022). Another group of filler membrane materials is ZIF. A series of DCMD experiments in combination with numerical modelling using JAVA software were conducted to study the water flux and rejection rate of simulated solutions containing salts and dyes and the mass transfer behaviour of the MD process. A composite ZIF doped in PVDF-co-HFP nanofibrous membrane synthesized by the electrospinning technique

was used. The salts and dye solutions were prepared by mixing acid red, acid yellow, methylene blue, and crystal violet with NaCl. The ZIF/PVDF-co-HFP membrane showed high permeate flux (19.2 L $m^{-2}{\cdot}h^{-1}$) and a dye rejection ≥99.99% compared to the pristine PVDF-co-HFP membrane and a commercial PVDF membrane. To model the DCMD process, the membrane was orderly divided into N different blocks per 1 cm. The TPC of different nanofibres was theoretically calculated by determining the saturated and unsaturated vapour pressure of the first membrane block using the Antoine equation and a partial pressure equation of non-ideal binary mixtures (Huang et al., 2022; Yun et al., 2006). Also, by calculating the membrane water permeation by iteration, the water permeation coefficient of different ZIF/PVDF-co-HFP membranes was obtained. The water flux was simulated by dividing the membrane into 30 blocks, each with a length of 1 mm, and by calculating the flux in every block. The model showed good accuracy with respect to the experimental and simulated water flux. The negatively charged acid red and acid yellow dyes were effectively rejected compared to the methylene blue and crystal violet dyes due to the negative charge characteristics of the ZIF/PVDF-co-HFP nanofibrous membrane (Huang et al., 2022).

Textile industries release high temperature wastewater that can potentially be treated by MD processes. In this process, the heat already present in the discharge solution is used to provide the energy for MD processes (Pavithra S.K P and Jaikumar S.R P, 2019). However, one of the main limitations of industrial wastewater is the presence of organic compounds, softeners and levelling agents, such as surfactants, which can cause fouling or wetting of the membrane. The presence of surfactants reduce the surface tension and thus, the LEP of the membrane and impact the MD performance (Calabro et al., 1991). An agarose hydrogel thin layer attached to the surface of a hydrophobic porous PTFE membrane was used to investigate the impact of hydrogel properties on the membrane wetting during the MD treatment of polyester fabric dyeing wastewater exposed to different types of surfactants. The agarose is a linear polymer with a molecular weight of 120 kDa (Lin et al., 2015). According to the reported findings, the unmodified MD membrane decreased flux rapidly, and the conductivity increased in a short period of time, indicating the occurrence of membrane wetting due to the presence of the surfactant. However, with the PTFE-agarose treated membrane, the flux and the conductivity remained unchanged for 24 h. The agarose layer repelled the hydrophobic moiety of the surfactant, which in turn prevented the formation of micelle; therefore, preventing the surfactant from penetrating through the hydrogel layer to cause membrane wetting (Lin et al., 2015). Furthermore, the flux of the MD process using the PTFE-agarose treated membrane is not limited by mass transfer through the hydrogel (Lin et al., 2015). The flux variation was attributed to the lower heat transfer coefficient of the protective layer, which reduces the vaporization temperature, causing flux decline while improving membrane resistance to wetting. Increasing the surface area of the membrane or the thermal conductivity of the protective hydrogen layer, the MD efficiency for dyeing wastewater treatment remain the same (Lin et al., 2015; Yan et al., 2022). Fig. 10 shows the temperature profile of the PTFE-agarose protected membrane, the rejection of the hydrophobic moiety of the surfactant by the hydrogen protective layer, and the penetration of surfactant micelles through the hydrogen layer during the MD process, respectively.

The micelle formation was explained by Musnicky et al. (2011) by conducting studies on the gradient diffusion of surfactants such as ionic sodium dodecyl sulfate (SDS) micelles in agarose gel, and by comparing the results with published theories (Musnicki et al., 2011). The study used holographic interferometry to measure the gradient diffusion coefficient at different sodium chloride, gel, and surfactant concentrations. Based on the reported findings, micelle diffusivity increased linearly with surfactant concentration with decreasing sodium chloride and gel concentrations. This behaviour suggested decreasing micelle-micelle electrostatic interactions with increasing sodium chloride concentrations. The concentration effect is quite strong for charged solutes, thus

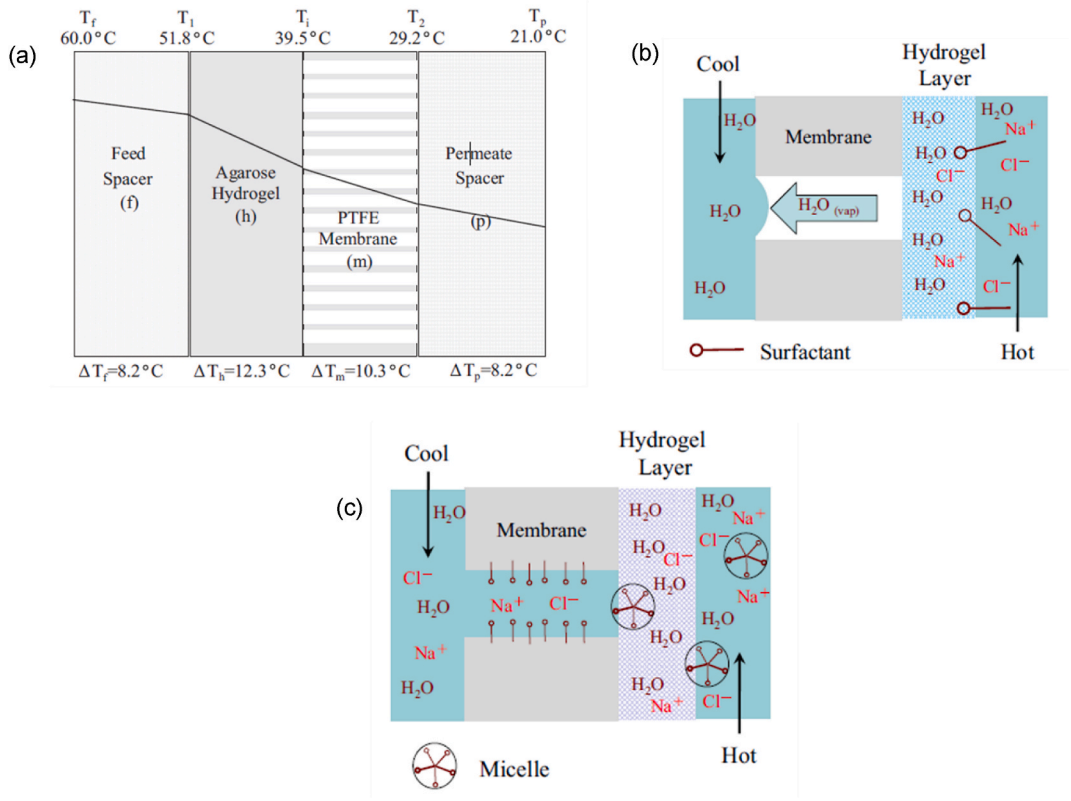

Fig. 10. (a) temperature profile of the PTFE-agarose protected membrane. The mechanism for (b) the rejection of the hydrophobic moiety of the surfactant by the hydrogen protective layer and (c) penetration of surfactant micelles through the hydrogen layer during the MD process (Lin et al., 2015).

doubling micelle diffusion coefficient relative to its value in the same gel at infinite dilution. The study compared the extrapolated, infinite-dilution diffusion coefficients and the rate at which the micelle diffusivity increased with surfactant concentration with predictions of previously published theories in which the micelles are treated as charged, colloidal spheres and the gel as a Brinkman medium. The experimental data and theoretical predictions were in good agreement (Musnicki et al., 2011).

In a research study, micellar enhanced ultrafiltration (MEUF) integrated with VMD was used to remove methylene blue from aqueous solutions and treat the MEUF reject to increase water recovery (Parakala et al., 2019). A theoretical model based on modified resistances in series was used to determine the effect of feed dye concentration, surfactant concentration, and feed pressure on the flux of the MEUF process. The CFD model was used to predict the LEP of the VMD membranes in the presence of the dye. Sodium dodecyl sulfate and sodium chloride were added to the dye solutions as anionic surfactant and electrolyte, respectively, to promote micelle formation. A polyethersulfone (PES) membrane loaded with activated carbon was used in the UF process, and a tetraethyl orthosilicate crosslinked polysulfone (PS) membrane was used in the VMD process to treat the UF retentate. The resistance in series model predicted the operating parameters and generate a minimum error between predicted and simulated UF fluxes. The computational model provided an insight into the movement of fluid-fluid interface inside the pores of the membrane. The MEUF-VMD integrated system provided pure water while the two membranes remained stable. The system can operate in continuous mode by increasing the surface area of the VMD membrane to match the MEFU flux. The hybrid system could treat wastewater generated by the distillery, starch, pharmaceutical, and tannery industry (Parakala et al., 2019).

6. Application of machine learning and artificial intelligence in MD

Optimizing the MD process towards removal of dyes from water is experimentally time-consuming and expensive requiring the selection of many parameters (Ohale et al., 2022; Silva et al., 2020). The application of methods shortening process time, increasing efficiency, and reducing the cost of the process is key. One of the most promising approaches involves the use of AI to model and optimize dye pollution removal (Sathishkumar et al., 2023; Fan et al., 2018; Aghilesh et al., 2023). The term AI covers many types of algorithms. Recently, attempts have been made to apply some algorithms to predict the optimal course of the water treatment process. Although AI has been evaluated in various treatment processes towards removal of dyes from wastewater, it is rarely reported in MD. Therefore, the AI-assisted MD in dye wastewater treatment processes is recommended.

The most commonly applied AI in environmental sciences and biotechnology challenges are the classical neural networks, namely artificial neuron networks (ANNs) (Holzinger et al., 2023). They are based on the model of a perceptron neuron known as the binary linear classifier (Krogh, 2008). In general, neural networks are the computational tools enabling computers to learn some patterns by analysing training datasets. In the case of the perceptron, the input data enter the neuron model with appropriately assigned weights, they are summed up (i.e., they form the so-called weighted sum) and after applying the activation function (also known as step function) return the desired result. The ANNs were used to predict the removal efficiency of the methylene blue (Sadek and Mostafa, 2023). The neural network consisting of ten hidden layers was applied (Elshfai et al., 2022). The feedforward backpropagation algorithm was used for the classification tasks (Mahmoud et al., 2019). The proposed approach can be successfully applied to maximize the methylene blue removal with nano zero-valent aluminum (nZVAI). The ANNs with one hidden layer consisting of ten perceptrons (created with MATLAB, 2019b packed software) were applied to the prediction of the CR adsorption (Ahmad Aftab et al., 2023). Notably, AI-based algorithms have the potential to be used as a supporting tool in the planning and development of more efficient dye removal.

Another AI-based algorithm applied in the dye removal process is Support Vector Machines (SVM). It is the concept of decision space, i.e., multidimensional hyperplane space separating cases belonging to different classes. The decision space is divided by building boundaries separating objects included in different patterns (Noble, 2006). The SVM-based algorithm predicts the methylene blue removal rate with high accuracy, and was therefore applied to optimize the congo red adsorption (Subramanian et al., 2023). The comparison of the AI-based algorithmic performance in the field of dye removal considering algorithms type, their application field, accuracy, the proportions of training sets, and inputs and outputs parameters is summarised in Table 4. Interestingly, AI-based algorithms are noteworthy computational tools in the context of predicting important parameters of the pollution removal process.

7. Challenges and prospects, and perspectives

Utilization of MD in treating the dye wastewater offers various benefits such as high removal efficiency and the process versatility in handling a wide range of dyes in various compositions. Also, MD is particularly effective in treating dye-contaminated waters under high salinity and elevated temperatures. During the process treatment, high-quality water is produced. Among other things, it provides a promising sustainable solution towards treatment of dye-contaminated wastewater due to low energy requirements. Also, advancements in membrane materials and optimization of the process performance and scalability pave a way to wide adoption of this process towards future dye-wastewater treatment. However, to ensure full adoption at industrial scale, various challenges including membrane wetting, fouling and requirement of high capital costs must be overcome. Also, system design with improved efficiency is imperative to minimize the process operating costs while promoting the attractiveness of the technology to dye wastewater treatment.

There are many challenges limiting long-term operation and costs of water processing. One of the problematic factors is the membrane fouling (Mokhtara et al., 2016; Laqbaqbi et al., 2019b). Besides advantages like high rejection of dissolved ions, low applied pressure, high permeate flux, processability on the commercial scale, and low operating temperature, the MD water processing remains energy intensive with high conductive heat loss (Buckner et al., 2016; Mokhtar et al., 2014b). According to the reported literature, the AGMD is more suitable to textile wastewater treatment compared to DCMD for its simplicity, higher thermal efficiencies, and low risk of the TP (Goh et al., 2022). Nevertheless, this method results in low flux compared to other configurations. Although high fluxes are reported in DCMD, the process is limited to high membrane wettability. The SGMD requires more complex setups limiting its broad use in contrast to other configurations. Also, SGMD has a higher risk of TP.

Development of scalable processes to fabricate membranes incorporated with nanoporous materials such as zeolites, metal-organic materials, and 2D materials is imperative. Currently, these membranes are at a relatively low technology readiness level. Interfacial polymerization is the most used technique to form ultrathin membranes for gas and water treatment. A recent review discusses opportunities and challenges associated with practical application of porous material at large scale and commercialization of membranes modified with nanoporous materials (Castro-Munoz et al., 2023). Some of the determining factors for potential commercialization include membrane selectivity and permeability, membrane synthesis cost, long-term stability and process reproducibility. Therefore, there is need to develop scalable fabrication methods with reproducible membranes in terms of structure and separation performance.

Many sources demonstrate application of MD on the model and real

Table 4
The comparison of the AI-based algorithms applied in dye removal.

Application field	AI-based algorithm type	Accuracy	Training/testing/validation sets [%]	Inputs parameters	Outputs parameters	Ref.
Prediction of the MB removal efficiency	ANNs	0.97	60.00/20.00/20.00	Parameters (residence time, initial MB concentration, temperature, pH, stirring rate, nZVI dosage, the concentration of two detergents: Ariel and Vanish, and the concentration of three salts: NaCl, Na_2CO_3, and Na_2SO_4)	MB removal efficiency	Sadek and Mostafa (2023)
Prediction of the alizarin red S removal efficiency	ANNs	0.99	lack of information	4 parameters (pH, the initial Alizarin concentration in the feed, the extractant volume percentage in the organic phase, and the fluid flow rate)	Alizarin red S removal efficiency	Hosseini and Rahimi (2023)
Prediction of the CR adsorption	ANNs	0.99	lack of information	4 parameters (starting concentration, pH, temperature, time)	adsorp-tion capacity of CR	Ahmad Aftab et al. (2023)
Prediction of the malachite green	ANNs	0.99	lack of information	10 parameters (catalyst type, reaction time, light intensity, initial concentration, catalyst loading, solution pH, humic acid concentration, anions, surface area, and pore volume of various photocatalysts)	Malachite green degradation efficiency	Jaffari et al. (2023)
Prediction of the CR adsorption	SVM	0.99	lack of information	4 parameters (starting concentration, pH, temperature, time)	adsorp-tion capacity of CR	Ahmad Aftab et al. (2023)
Prediction of the MB degradations efficiency	SVM	0.94	85.00/15.00/0.00	4 parameters (pH, dye concentration, photocatalyst dose and irradiation exposure time)	MB removal rate (%)	Subramanian et al. (2023)

MB: methylene blue, ANNs: artificial neuron networks, SVM: Support vector machine.

wastewater solutions containing different concentration of dyes, where the application is limited to the solutions below or equal 100 ppm of certain dye. The increase in dye concentration causes a decay in permeate flux (Tolentino Filho et al., 2022). Another challenge is surface tension of the membrane and wetting in presence of surfactants commonly present in textile wastewaters (Yang et al., 2021; Nthunya et al., 2019d). Formation of cohesive interactions between the hydrophilic groups of surfactant molecules in the feed affect permeation flux, thus necessitating the wetting investigation during MD treatment of textile wastewater (Dow et al., 2017; Silva et al., 2020; Nthunya et al., 2019d). Besides studies in the presence of surfactants, the improvement of the surface properties of the membrane towards superhydrophobicity is desired. Also, it is important to investigate steady state and operation times for each techniques (Silva et al., 2020). Just in the same way, MD treatment of dyes requires effective and universal analytical models to understand the heat and mass transfer during treatment of specific dyes. This is particularly important in treatment of environmental wastewater characterised by varying pH, salinity, and presence of different chemicals (Madalosso et al., 2021). Indeed, literature refers to mathematical models developed for certain membrane configurations (flat sheet, spiral or hollow fibre) used in MD pilot units to predict mass fluxes and compare them with measured water vapour fluxes (Alsaadi et al., 2013). However, extensive research is required.

To address the thermal efficiencies in MD, the research has geared towards evaluation of photothermal membrane distillation (PMD). This was encouraged by the large energy consumption with low thermal efficiency impeding the process application at energy off-grid areas (Li et al., 2020b; Politano et al., 2017). The PMD utilizes the solar energy modification of the membrane to heat the feed solution by photothermal materials in situ. Technically, the photothermal materials are embedded into the membrane to generate the solar-based thermal energy. The temperature of the feed at the membrane interface is higher than the temperature of the bulk feed, thus enabling the large temperature difference and therefore the high vapour pressure gradient (Razaqpur et al., 2021). Various materials evaluated to convert light to heat include TiO_2, molybdenum disulfide (MoS_2), and MXenes (Ti_3C_2), CNTs, GO, and RGO (Jun et al., 2019). Zhang et al. (2023) used carbonized lotus root as an alternative cost effective photothermal materials to induce steam from the seawater via a solar simulator. The distillation process presented the flux of 0.90 kg m^{-2}•h^{-1} and GOR of 0.61 under 1 kWm^{-2} illumination (Zhang et al., 2023). Although utilization of photothermal materials have opened research direction towards cost-effective desalination processes, treatment of dye wastewater via PMD is rarely reported.

8. Conclusions

Membrane distillation (MD) emerged as an effective promising technology capable of treating industrial wastewater including textile. Previously reported studies advanced significant strides of MD process optimization, with a specific focus on membrane properties and operating parameters to improve rate of water recovery and dye removal efficiency. The MD facilitates water and dye separation through vapour-phase transport mechanisms where the porous hydrophobic membrane permit passage of water vapour and volatile compounds while retaining the dye molecules. The current study comprehensively reviewed the MD treatment of various classes of dyes such as azo, reactive, and anthraquinone. Nonetheless, process challenges including membrane fouling, and energy optimizations require further considerations to enable practical implementation in textile wastewater management. To address these challenges, innovative approaches should focus on fouling mitigation strategies, improved membrane properties through surface modification. Thermal energy consumption requires critical attention in MD to assess its economic viability and environmental sustainability. As per previously reported studies, MD operation using low-grade or waste heat reduces the operations costs. However, some studies challenge the phenomenon of cost reduction upon use of low-grade energy or waste heat. For these reasons, research is geared towards module designs and fabrication of low-thermal conducting membranes. Also, in situ detection of membrane fouling is required to enable an immediate mitigation. Among other technologies, artificial intelligence (AI) emerged as the modelling technology to improve process efficiency. However, AI evaluation in MD dye removal requires extensive research. Similarly, the emphasised need to use sustainable and environmentally friendly dye removal technologies, MD provides a promising avenue to address the water pollution caused by growing textile industries. Technically, the MD aligns with required principles of energy efficiency and zero liquid discharge (ZLD). Upon further research and development efforts, coupled with advancements in process optimization, MD presented a great potential to treat dye-contaminated sources in a cost-effective and eco-friendly manner, thus ensuring cleaner and more sustainable water resources.

CRediT authorship contribution statement

Lebea N. Nthunya: Writing – review & editing, Writing – original draft, Visualization, Validation, Supervision, Resources, Project administration, Methodology, Investigation, Formal analysis, Conceptualization. **Kok Chung Chong:** Investigation, Writing – original draft. **Soon Onn Lai:** Investigation, Writing – original draft. **Woei Jye Lau:** Formal analysis, Investigation, Validation, Writing – original draft, Writing – review & editing. **Eduardo Alberto López-Maldonado:** Formal analysis, Investigation, Validation, Writing – original draft, Writing – review & editing. **Lucy Mar Camacho:** Formal analysis, Investigation, Validation, Writing – original draft, Writing – review & editing. **Mohammad Mahdi A. Shirazi:** Validation, Writing – original draft. **Aamer Ali:** Writing – original draft. **Bhekie B. Mamba:** Formal analysis, Supervision. **Magdalena Osial:** Writing – original draft. **Paulina Pietrzyk-Thel:** Writing – original draft. **Agnieszka Pregowska:** Writing – original draft. **Oranso T. Mahlangu:** Data curation, Formal analysis, Investigation, Validation, Writing – original draft, Writing – review & editing.

Declaration of competing interest

The authors declare that they have no known competing financial interests or personal relationships that could have appeared to influence the work reported in this paper.

Data availability

Data will be made available on request.

Acknowledgments

The authors would like to thank the University of the Witwatersrand and National Research Foundation (NRF-grant number: 132724) for funding this research work.

References

Abdel-Karim, A., Leaper, S., Skuse, C., Zaragoza, G., Gryta, M., Gorgojo, P., 2021. Membrane cleaning and pretreatments in membrane distillation – a review. Chem. Eng. J. 422, 129696 https://doi.org/10.1016/j.cej.2021.129696.

Adel, M., Nada, T., Amin, S., Anwar, T., Mohamed, A.A., 2022. Characterization of fouling for a full-scale seawater reverse osmosis plant on the Mediterranean sea: membrane autopsy and chemical cleaning efficiency. Groundw. Sustain. Dev. 16, 100704 https://doi.org/10.1016/j.gsd.2021.100704.

Afsari, M., Shirazi, M.M.A., Ghorbani, A.H., Sayar, O., Shon, H.K., Tijing, L.D., 2023. Triple-layer nanofiber membrane with improved energy efficiency for treatment of hypersaline solution via membrane distillation. J. Environ. Chem. Eng. 11, 110638 https://doi.org/10.1016/j.jece.2023.110638.

Aghilesh, K., Kumar, A., Agarwal, S., Garg, M.C., Joshi, H., 2023. Use of artificial intelligence for optimizing biosorption of textile wastewater using agricultural waste. Environ. Technol. 44, 22–34. https://doi.org/10.1080/09593330.2021.1961874.

Ahmad Aftab, R., Zaidi, S., Aslam Parwaz Khan, A., Arish Usman, M., Khan, A.Y., Tariq Saeed Chani, M., Asiri, A.M., 2023. Removal of Congo red from water by adsorption onto activated carbon derived from waste black cardamom peels and machine learning modeling. Alex. Eng. J. 71, 355–369. https://doi.org/10.1016/j.aej.2023.03.055.

Ahmad, M.Z., Pelletier, H., Martin-gil, V., Castro-muñoz, R., Fila, V., 2018. Chemical crosslinking of 6FDA-ODA and 6FDA-ODA: DABA for improved CO2/CH4 separation. Membranes 8, 67. https://doi.org/10.3390/membranes8030067.

Ahmed, M.A., Amin, S., Mohamed, A.A., 2023. Fouling in reverse osmosis membranes: monitoring, characterization, mitigation strategies and future directions. Heliyon 9, e14908. https://doi.org/10.1016/j.heliyon.2023.e14908. Contents.

Aijaz, M.O., Karim, M.R., Othman, M.H.D., Samad, U.A., 2023. Anti-fouling/wetting electrospun nanofibrous membranes for membrane distillation desalination: a comprehensive review. Desalination 553, 116475. https://doi.org/10.1016/j.desal.2023.116475.

Al-Sharif, S., Albeirutty, M., Cipollina, A., Micale, G., 2013. Modelling flow and heat transfer in spacer-filled membrane distillation channels using open source CFD code. Desalination 311, 103–112. https://doi.org/10.1016/j.desal.2012.11.005.

Al-Tohamy, R., Ali, S.S., Li, F., Okasha, K.M., Mahmoud, Y.A.G., Elsamahy, T., Jiao, H., Fu, Y., Sun, J., 2022. A critical review on the treatment of dye-containing wastewater: Ecotoxicological and health concerns of textile dyes and possible remediation approaches for environmental safety. Ecotoxicol. Environ. Saf. 231, 113160 https://doi.org/10.1016/j.ecoenv.2021.113160.

Alawad, S.M., Khalifa, A.E., 2021. Performance and energy evaluation of compact multistage air gap membrane distillation system: an experimental investigation. Sep. Purif. Technol. 268, 118594 https://doi.org/10.1016/j.seppur.2021.118594.

Ali, A., Aimar, P., Drioli, E., 2015. Effect of module design and flow patterns on performance of membrane distillation process. Chem. Eng. J. 277, 368–377. https://doi.org/10.1016/j.cej.2015.04.108.

Ali, A., Quist-Jensen, C.A., Macedonio, F., Drioli, E., 2016. Optimization of module length for continuous direct contact membrane distillation process. Chem. Eng. Process. Process Intensif. 110, 188–200. https://doi.org/10.1016/j.cep.2016.10.014.

Ali, A., Tsai, J.H., Tung, K.L., Drioli, E., Macedonio, F., 2018. Designing and optimization of continuous direct contact membrane distillation process. Desalination 426, 97–107. https://doi.org/10.1016/j.desal.2017.10.041.

Ali, A., Criscuoli, A., Macedonio, F., Drioli, E., 2019. A comparative analysis of flat sheet and capillary membranes for membrane distillation applications. Desalination 456, 1–12. https://doi.org/10.1016/j.desal.2019.01.006.

Ali, A., Agha Shirazi, M.M., Nthunya, L., Castro-Muñoz, R., Ismail, N., Tavajohi, N., Zaragoza, G., Quist-Jensen, C.A., 2024. Progress in module design for membrane distillation. Desalination 581, 117584. https://doi.org/10.1016/j.desal.2024.117584.

Alkhatib, A., Ayari, M.A., Hawari, A.H., 2021. Fouling mitigation strategies for different foulants in membrane distillation. Chem. Eng. Process. - Process Intensif. 167, 108517 https://doi.org/10.1016/j.cep.2021.108517.

Alsaadi, A.S., Ghaffour, N., Li, J.D., Gray, S., Francis, L., Maab, H., Amy, G.L., 2013. Modeling of air-gap membrane distillation process: a theoretical and experimental study. J. Memb. Sci. 445, 53–65. https://doi.org/10.1016/j.memsci.2013.05.049.

Alsawaftah, N., Abuwatfa, W., Darwish, N., Husseini, G., 2021. A comprehensive review on membrane fouling: mathematical modelling. prediction, diagnosis, and mitigation, Water (Switzerland) 13. https://doi.org/10.3390/w13091327.

An, A.K., Guo, J., Jeong, S., Lee, E.J., Tabatabai, S.A.A., Leiknes, T.O., 2016. High flux and antifouling properties of negatively charged membrane for dyeing wastewater treatment by membrane distillation. Water Res. 103, 362–371. https://doi.org/10.1016/j.watres.2016.07.060.

An, A.K., Guo, J., Lee, E.J., Jeong, S., Zhao, Y., Wang, Z., Leiknes, T.O., 2017. PDMS/PVDF hybrid electrospun membrane with superhydrophobic property and drop impact dynamics for dyeing wastewater treatment using membrane distillation. J. Memb. Sci. 525, 57–67. https://doi.org/10.1016/j.memsci.2016.10.028.

Baghel, R., Kalla, S., Upadhyaya, S., Chaurasia, S.P., Singh, K., 2020. CFD modeling of vacuum membrane distillation for removal of Naphthol blue black dye from aqueous solution using COMSOL multiphysics. Chem. Eng. Res. Des. 158, 77–88. https://doi.org/10.1016/j.cherd.2020.03.016.

Banat, F., A-asheh, S., Qtaishat, M., 2005a. Treatment of waters colored with methylene blue dye by vacuum membrane distillation. Desalination 174, 87–96. https://doi.org/10.1016/j.desal.2004.09.004.

Banat, F., Al-Asheh, S., Qtaishat, M., 2005b. Treatment of waters colored with methylene blue dye by vacuum membrane distillation. Desalination 174, 87–96. https://doi.org/10.1016/j.desal.2004.09.004.

Banat, F., Jwaied, N., Rommel, M., Koschikowski, J., Wieghaus, M., 2007. Desalination by a "compact SMADES" autonomous solarpowered membrane distillation unit. Desalination 217, 29–37. https://doi.org/10.1016/j.desal.2006.11.028.

Benkhaya, S., Souad, M., El Harfi, A., 2020a. A review on classifications , recent synthesis and applications of textile dyes. Inorg. Chem. Commun. 115, 107891 https://doi.org/10.1016/j.inoche.2020.107891. Contents.

Benkhaya, S., Souad, M., El Harfi, A., 2020b. A review on classifications , recent synthesis and applications of textile dyes. Inorg. Chem. Commun. 115, 107891 https://doi.org/10.1016/j.inoche.2020.107891.

Benkhaya, S., Lgaz, H., Tang, H., Altaee, A., Haida, S., Vatanpour, V., Xiao, Y., 2023. Investigating the effects of polypropylene-TiO2 loading on the performance of polysulfone/polyetherimide ultrafiltration membranes for azo dye removal: experimental and molecular dynamics simulation. J. Water Process Eng. 56, 104317 https://doi.org/10.1016/j.jwpe.2023.104317.

Buckner, C.A., Lafrenie, R.M., Dénommée, J.A., Caswell, J.M., Want, D.A., Gan, G.G., Leong, Y.C., Bee, P.C., Chin, E., Teh, A.K.H., Picco, S., Villegas, L., Tonelli, F., Merlo, M., Rigau, J., Diaz, D., Masuelli, M., Korrapati, S., Kurra, P., Puttugunta, S., Picco, S., Villegas, L., Tonelli, F., Merlo, M., Rigau, J., Diaz, D., Masuelli, M., Tascilar, M., de Jong, F.A., Verweij, J., Mathijssen, R.H.J., 2016. Membrane distillation: Basics, advances, and applications. In: Adv. Membr. Technol. INTECH, pp. 1–21. https://www.intechopen.com/books/advanced-biometric-technologies/liveness-detection-in-biometrics.

Calabro, V., Drioli, E., Matera, F., 1991. Membrane distillation in the textile wastewater treatment. Desalination 83, 209–224, 10.1016/0011-9164(91)85096-D.

Camacho, L.M., Dumée, L., Zhang, J., de Li, J., Duke, M., Gomez, J., Gray, S., 2013. Advances in membrane distillation for water desalination and purification applications. Water 5, 94–196. https://doi.org/10.3390/w5010094.

Castro-Munoz, R., V Agrawal, K., Lai, Z., Coronas, J., 2023. Towards large-scale application of nanoporous materials in membranes for separation of energy-relevant gas mixtures. Sep. Purif. Technol. 308, 122919 https://doi.org/10.1016/j.seppur.2022.122919.

Charfi, A., Tibi, F., Kim, J., Hur, J., Cho, J., 2021. Organic fouling impact in a direct contact membrane distillation system treating wastewater: experimental observations and modeling approach. Membranes 11, 1–12. https://doi.org/10.3390/membranes11070493.

Chernyshov, M.N., Meindersma, G.W., de Haan, A.B., 2005. Comparison of spacers for temperature polarization reduction in air gap membrane distillation. Desalination 183, 363–374. https://doi.org/10.1016/j.desal.2005.04.029.

Chidambaram, T., Oren, Y., Noel, M., 2015. Fouling of nanofiltration membranes by dyes during brine recovery from textile dye bath wastewater. Chem. Eng. J. 262, 156–168. https://doi.org/10.1016/j.cej.2014.09.062.
Chimanlal, I., Nthunya, L.N., Mahlangu, O.T., Kirkebæk, B., Ali, A., Quist-jensen, C.A., Richards, H., 2023a. Nanoparticle-enhanced PVDF flat-sheet membranes for seawater desalination in direct contact membrane distillation. Membranes 13, 1–17. https://doi.org/10.3390/membranes13030317.
Chimanlal, I., Nthunya, L.N., Quist-Jensen, C., Richards, H., 2023b. Resource recovery from acid mine drainage in membrane distillation crystallization. Front. Membr. Sci. Technol. 2, 1–10. https://doi.org/10.3389/frmst.2023.1247276.
Choudhury, M.R., Anwar, N., Jassby, D., Rahaman, M.S., 2019. Fouling and wetting in the membrane distillation driven wastewater reclamation process – a review. Adv. Colloid Interface Sci. 269, 370–399. https://doi.org/10.1016/j.cis.2019.04.008.
Christie, K.S.S., Horseman, T., Lin, S., 2020. Energy efficiency of membrane distillation: Simplified analysis, heat recovery, and the use of waste-heat. Environ. Int. 138 https://doi.org/10.1016/j.envint.2020.105588.
Cosme, J.R.A., Castro-mun, R., 2023. Recent Advances in Nanocomposite Membranes for Organic Compound Remediation from Potable Waters 112–132. https://doi.org/10.1002/cben.202200017.
Criscuoli, A., Zhong, J., Figoli, A., Carnevale, M.C., Huang, R., Drioli, E., 2008a. Treatment of dye solutions by vacuum membrane distillation. Water Res. 42, 5031–5037. https://doi.org/10.1016/j.watres.2008.09.014.
Criscuoli, A., Zhong, J., Figoli, A., Carnevale, M.C., Huang, R., Drioli, E., 2008b. Treatment of dye solutions by vacuum membrane distillation. Water Res. 42, 5031–5037. https://doi.org/10.1016/j.watres.2008.09.014.
Dow, N., Villalobos García, J., Niadoo, L., Milne, N., Zhang, J., Gray, S., Duke, M., 2017. Demonstration of membrane distillation on textile waste water assessment of long term performance, membrane cleaning and waste heat integration. Environ. Sci. Water Res. Technol. 3, 433–449. https://doi.org/10.1039/c6ew00290k.
Drioli, E., Matera, F., 1991. Membrane distillation in the textile wastewater treatment. Desalination 83, 209–224.
Du, S., Zhao, P., Wang, L., He, G., Jiang, X., 2023. Progresses of advanced anti-fouling membrane and membrane processes for high salinity wastewater treatment. Results Eng 17, 100995. https://doi.org/10.1016/j.rineng.2023.100995.
Duong, H.C., Cooper, P., Nelemans, B., Cath, T.Y., Nghiem, L.D., 2015. Optimising thermal efficiency of direct contact membrane distillation by brine recycling for small-scale seawater desalination. Desalination 374, 1–9. https://doi.org/10.1016/j.desal.2015.07.009.
Duong, H.C., Cooper, P., Nelemans, B., Cath, T.Y., Nghiem, L.D., 2016. Evaluating energy consumption of air gap membrane distillation for seawater desalination at pilot scale level. Sep. Purif. Technol. 166, 55–62. https://doi.org/10.1016/j.seppur.2016.04.014.
El, K., Isam, K., Raed, J., 2020. Numerical simulation and evaluation of spacer - filled direct contact membrane distillation module. Appl. Water Sci. 10, 1–17. https://doi.org/10.1007/s13201-020-01261-9.
Elgharbi, S., Boubakri, A., Bouguecha, S., Bilel, H., Matalka, S.I., Hafiane, A., 2024. Membrane distillation for methylene blue dye removal from wastewater: Investigating process optimization and membrane wettability. Arab. J. Sci. Eng. https://doi.org/10.1007/s13369-024-08756-6.
Elhenawy, Y., Bassyouni, M., Fouad, K., Sandid, A.M., Abu-Zeid, M.A.E.R., Majozi, T., 2023. Experimental and numerical simulation of solar membrane distillation and humidification – dehumidification water desalination system. Renew. Energy 215, 118915. https://doi.org/10.1016/j.renene.2023.118915.
Elmarghany, M.R., El-Shazly, A.H., Salem, M.S., Sabry, M.N., Nady, N., 2019. Thermal analysis evaluation of direct contact membrane distillation system. Case Stud. Therm. Eng. 13, 100377 https://doi.org/10.1016/j.csite.2018.100377.
Elshfai, M.M., Hassan, R.G., Mahmoud, A.S., 2022. Reduction of biological contaminants from municipal wastewater by encapsulated nZVI in alginate (Ag) polymer: reduction mechanism with artificial intelligence approach. Key Eng. Mater. 921, 173–189. https://doi.org/10.4028/p-pk7pa4.
Elwardany, R.E., Shokry, H., Mustafa, A.A., Ali, A.E., 2023. Influence of the prepared activated carbon on cellulose acetate for malachite green dye removal from aqueous solution. Macromol. Res. 31, 1043–1060. https://doi.org/10.1007/s13233-023-00187-w.
Eykens, L., Hitsov, I., De Sitter, K., Dotremont, C., Pinoy, L., Nopens, I., Van der Bruggen, B., 2016. Influence of membrane thickness and process conditions on direct contact membrane distillation at different salinities. J. Memb. Sci. 498, 353–364. https://doi.org/10.1016/j.memsci.2015.07.037.
Eykens, L., De Sitter, K., Dotremont, C., Pinoy, L., Van der Bruggen, B., 2017. Membrane synthesis for membrane distillation: a review. Sep. Purif. Technol. 182, 36–51. https://doi.org/10.1016/j.seppur.2017.03.035.
Fan, M., Hu, J., Cao, R., Ruan, W., Wei, X., 2018. A review on experimental design for pollutants removal in water treatment with the aid of artificial intelligence. Chemosphere 200, 330–343. https://doi.org/10.1016/j.chemosphere.2018.02.111.
Fortunato, L., Elcik, H., Blankert, B., Ghaffour, N., Vrouwenvelder, J., 2021. Textile dye wastewater treatment by direct contact membrane distillation: membrane performance and detailed fouling analysis. J. Memb. Sci. 636, 119552 https://doi.org/10.1016/j.memsci.2021.119552.
Fried, R., Oprea, I., Fleck, K., Rudrof, F., 2022. Biogenic colourants in the textile industry – a promising and sustainable alternative to synthetic dyes. Green Chem. 24, 13–35. https://doi.org/10.1039/d1gc02968a.
Gao, L., Zhang, J., Gray, S., De Li, J., 2019. Influence of PGMD module design on the water productivity and energy efficiency in desalination. Desalination 452, 29–39. https://doi.org/10.1016/j.desal.2018.10.005.
García, J.V., Dow, N., Milne, N., Zhang, J., Naidoo, L., Gray, S., Duke, M., 2018. Membrane distillation trial on textile wastewater containing surfactants using hydrophobic and hydrophilic-coated polytetrafluoroethylene (PTFE) membranes. Membranes 8, 1–15. https://doi.org/10.3390/membranes8020031.
Ge, Q., Wang, P., Wan, C., Chung, T.-S., 2012. Polyelectrolyte-promoted forward osmosis – membrane distillation (FO – MD) hybrid process for dye wastewater treatment. Environ. Sci. Technol. 46, 6236–6243. https://doi.org/10.1021/es300784h.
Goh, P.S., Wong, K.C., Ismail, A.F., 2022. Membrane technology: a versatile tool for saline wastewater treatment and resource recovery. Desalination 521, 115377. https://doi.org/10.1016/j.desal.2021.115377.
Gontarek-castro, E., Castro-muñoz, R., 2023. Membrane distillation assisting food production processes of thermally sensitive food liquid items: a review. Crit. Rev. Food Sci. Nutr. https://doi.org/10.1080/10408398.2022.2163223.
Gontarek-castro, E., Castro-Munoz, R., 2024. How to make membrane distillation greener: a review of environmentally friendly and sustainable aspects. Green Chem. 26, 164–185. https://doi.org/10.1039/d3gc03377e.
Gontarek-castro, E., Castro-muñoz, R., Lieder, M., 2022. New insights of nanomaterials usage toward superhydrophobic membranes for water desalination via membrane distillation: a review. Crit. Rev. Environ. Sci. Technol. 52, 2104–2149. https://doi.org/10.1080/10643389.2021.1877032.
Haddadi, B., Jordan, C., Miltner, M., Harasek, M., 2018. Membrane modeling using CFD: combined evaluation of mass transfer and geometrical influences in 1D and 3D. J. Memb. Sci. 563, 199–209. https://doi.org/10.1016/j.memsci.2018.05.040.
Hairom, N.H.H., Mohammad, A.W., Kadhum, A.A.H., 2014. Nanofiltration of hazardous Congo red dye: performance and flux decline analysis. J. Water Process Eng. 4, 99–106. https://doi.org/10.1016/j.jwpe.2014.09.008.
Haleem, A., Shafiq, A., Chen, S.Q., Nazar, M., 2023. A comprehensive review on adsorption, photocatalytic and chemical degradation of dyes and nitro-compounds over different kinds of porous and composite materials. Molecules 28. https://doi.org/10.3390/molecules28031081.
Hassan, M.M., Carr, C.M., 2018. A critical review on recent advancements of the removal of reactive dyes from dyehouse ef fl uent by ion-exchange adsorbents. Chemosphere 209, 201–219. https://doi.org/10.1016/j.chemosphere.2018.06.043.
Helaskoski, E., Suojalehto, H., Virtanen, H., Airaksinen, L., Outi, K., Aalto-Korte, M., Pesonen, Kristiina, 2014. Occupational asthma , rhinitis , and contact urticaria caused by oxidative hair dyes in hairdressers. Ann. Allergy Asthma Immunol. 112, 46–52. https://doi.org/10.1016/j.anai.2013.10.002.
Hidalgo, A.M., León, G., Gómez, M., Murcia, M.D., Gómez, E., Macario, J.A., 2020. Removal of different dye solutions: a comparison study using a polyamide nf membrane. Membranes 10, 1–16. https://doi.org/10.3390/membranes10120408.
Hitsov, I., De Sitter, K., Dotremont, C., Nopens, I., 2018. Economic modelling and model-based process optimization of membrane distillation. Desalination 436, 125–143. https://doi.org/10.1016/j.desal.2018.01.038.
Holkar, C.R., Jadhav, A.J., V Pinjari, D., Mahamuni, N.M., Pandit, A.B., 2016. A critical review on textile wastewater treatments : possible approaches. J. Environ. Manag. 182, 351–366.
Holzinger, A., Keiblinger, K., Holub, P., Zatloukal, K., Müller, H., 2023. AI for life: trends in artificial intelligence for biotechnology. N. Biotechnol. 74, 16–24. https://doi.org/10.1016/j.nbt.2023.02.001.
Homem, N.C., de Camargo Lima Beluci, N., Amorim, S., Reis, R., Vieira, A.M.S., Vieira, M.F., Bergamasco, R., Amorim, M.T.P., 2019. Surface modification of a polyethersulfone microfiltration membrane with graphene oxide for reactive dyes removal. Appl. Surf. Sci. 486, 499–507. https://doi.org/10.1016/j.apsusc.2019.04.276.
Hosseini, F., Rahimi, M., 2023. Experimental study and artificial intelligence modeling of dye removal in microfluidic systems. Chem. Eng. Technol. 46, 987–996. https://doi.org/10.1002/ceat.202300105.
Hou, J., Chen, Y., Shi, W., Bao, C., Hu, X., 2020. Graphene oxide/methylene blue composite membrane for dyes separation: formation mechanism and separation performance. Appl. Surf. Sci. 505, 144145 https://doi.org/10.1016/j.apsusc.2019.144145.
Hu, M., Mi, B., 2014. Layer-by-layer assembly of graphene oxide membranes via electrostatic interaction. J. Memb. Sci. 469, 80–87. https://doi.org/10.1016/j.memsci.2014.06.036.
Huang, Q., Huang, Y., Xiao, C., You, Y., Zhang, C., 2017. Self-cleaning function for vacuum membrane distillation. J. Memb. Sci. 534, 73–82. https://doi.org/10.1016/j.memsci.2017.04.015.
Huang, M., Song, J., Deng, Q., Mu, T., Li, J., 2022. Novel electrospun ZIF/PcH nanofibrous membranes for enhanced performance of membrane distillation for salty and dyeing wastewater treatment. Desalination 527, 115563. https://doi.org/10.1016/j.desal.2022.115563.
Huang, Y.H., Wang, M.J., Chung, T.S., 2023. Zwitterionic poly(sulfobetaine methacrylate-co-acrylic acid) assisted simultaneous anti-wetting and anti-fouling membranes for membrane distillation. Desalination 555, 116527. https://doi.org/10.1016/j.desal.2023.116527.
Ibrar, I., Yadav, S., Naji, O., Alanezi, A.A., Ghaffour, N., Déon, S., Subbiah, S., Altaee, A., 2022. Development in forward Osmosis-Membrane distillation hybrid system for wastewater treatment. Sep. Purif. Technol. 286, 120498 https://doi.org/10.1016/j.seppur.2022.120498.
Im, B.G., Francis, L., Santosh, R., Kim, W.S., Ghaffour, N., Kim, Y.D., 2022. Comprehensive insights into performance of water gap and air gap membrane distillation modules using hollow fiber membranes. Desalination 525, 1–15. https://doi.org/10.1016/j.desal.2021.115497.
Izquierdo-Gil, M.A., Jonsson, G., 2003. Factors affecting flux and ethanol separation performance in vacuum membrane distillation (VMD). J. Memb. Sci. 214, 113–130. https://doi.org/10.1016/S0376-7388(02)00540-9.
Jaffari, Z.H., Abbas, A., Lam, S.M., Park, S., Chon, K., Kim, E.S., Cho, K.H., 2023. Machine learning approaches to predict the photocatalytic performance of bismuth

ferrite-based materials in the removal of malachite green. J. Hazard Mater. 442, 130031 https://doi.org/10.1016/j.jhazmat.2022.130031.
Jain, A., Ahmad, M.Z., Link, A., Martin-gil, V., Castro-muñoz, R., Izak, P., Hintz, W., Fila, V., 2021. 6FDA-DAM: DABA Co-polyimide mixed matrix membranes with GO and ZIF-8 mixtures for effective CO2/CH4 separation. Nanomaterials 11, 668.
Julian, H., Ye, Y., Li, H., Chen, V., 2018. Scaling mitigation in submerged vacuum membrane distillation and crystallization (VMDC) with periodic air-backwash. J. Memb. Sci. 547, 19–33. https://doi.org/10.1016/j.memsci.2017.10.035.
Jun, Y.S., Wu, X., Ghim, D., Jiang, Q., Cao, S., Singamaneni, S., 2019. Photothermal membrane water treatment for two worlds. Acc. Chem. Res. 52, 1215–1225. https://doi.org/10.1021/acs.accounts.9b00012.
Kant, R., 2012. Textile dyeing industry an environmental hazard. Nat. Sci. 4, 22–26. https://doi.org/10.4236/ns.2012.41004.
Katheresan, V., Kansedo, J., Lau, S.Y., 2018. Efficiency of various recent wastewater dye removal methods : a review. J. Environ. Chem. Eng. 6, 4676–4697. https://doi.org/10.1016/j.jece.2018.06.060.
Khalifa, A.E., 2020. Flux enhanced water gap membrane distillation process-circulation of gap water. Sep. Purif. Technol. 231, 1–9. https://doi.org/10.1016/j.seppur.2019.115938.
Khayet, M., 2011. Membranes and theoretical modeling of membrane distillation: a review. Adv. Colloid Interface Sci. 164, 56–88. https://doi.org/10.1016/j.cis.2010.09.005.
Khayet, M., Cojocaru, C., 2012. Air gap membrane distillation: desalination, modeling and optimization. Desalination 287, 138–145. https://doi.org/10.1016/j.desal.2011.09.017.
Khayet, M., Cojocaru, C., Baroudi, A., 2012. Modeling and optimization of sweeping gas membrane distillation. Desalination 287, 159–166. https://doi.org/10.1016/j.desal.2011.04.070.
Khumalo, N.P., Nthunya, L.N., De Canck, E., Derese, S., Verliefde, A.R., Kuvarega, A.T., Mamba, B.B., Mhlanga, S.D., Dlamini, D.S., 2019. Congo red dye removal by direct membrane distillation using PVDF/PTFE membrane. Sep. Purif. Technol. 211, 578–586. https://doi.org/10.1016/j.seppur.2018.10.039.
Koschikowski, J., Wieghaus, M., Rommel, M., 2003. Solar thermal-driven desalination plants based on membrane distillation. Desalination 156, 295–304. https://doi.org/10.1016/S0011-9164(03)00360-6.
Koschikowski, J., Wieghaus, M., Rommel, M., Ortin, V.S., Suarez, B.P., Betancort Rodríguez, J.R., 2009. Experimental investigations on solar driven stand-alone membrane distillation systems for remote areas. Desalination 248, 125–131. https://doi.org/10.1016/j.desal.2008.05.047.
Krogh, A., 2008. What are artificial neural networks? Nat. Biotechnol. 26, 195–197. https://doi.org/10.1038/nbt1386.
Laqbaqbi, M., García-payo, M.C., Khayet, M., El Kharraz, J., Chaouch, M., 2019a. Application of direct contact membrane distillation for textile wastewater treatment and fouling study. Sep. Purif. Technol. 209, 815–825. https://doi.org/10.1016/j.seppur.2018.09.031.
Laqbaqbi, M., García-Payo, M.C., Khayet, M., El Kharraz, J., Chaouch, M., 2019b. Application of direct contact membrane distillation for textile wastewater treatment and fouling study. Sep. Purif. Technol. 209, 815–825. https://doi.org/10.1016/j.seppur.2018.09.031.
Leaper, S., Abdel-karim, A., Gad-allah, T.A., Gorgojo, P., 2019. Air-gap membrane distillation as a one-step process for textile wastewater treatment. Chem. Eng. J. 360, 1330–1340. https://doi.org/10.1016/j.cej.2018.10.209.
Lee, J.G., Jeong, S., Alsaadi, A.S., Ghaffour, N., 2018. Influence of high range of mass transfer coefficient and convection heat transfer on direct contact membrane distillation performance. Desalination 426, 127–134. https://doi.org/10.1016/j.desal.2017.10.034.
Li, H., Feng, X., 2019. Dye removal using hydrophobic polyvinylidene fluoride hollow fibre composite membrane by vacuum membrane distillation. Color. Technol. 135, 451–466. https://doi.org/10.1111/cote.12436.
Li, H., Feng, X., Shi, W., Zhang, H., Du, Q., Qin, L., Qin, X., 2019. Dye removal using hydrophobic polyvinylidene fluoride hollow fibre composite membrane by vacuum membrane distillation. Color. Technol. 135, 451–466. https://doi.org/10.1111/cote.12436.
Li, M., Li, K., Wang, L., Zhang, X., 2020a. Feasibility of concentrating textile wastewater using a hybrid forward osmosis-membrane distillation (FO-MD) process: performance and economic evaluation. Water Res. 172, 115488 https://doi.org/10.1016/j.watres.2020.115488.
Li, W., Chen, Y., Yao, L., Ren, X., Li, Y., Deng, L., 2020b. Fe3O4/PVDF-HFP photothermal membrane with in-situ heating for sustainable, stable and efficient pilot-scale solar-driven membrane distillation. Desalination 478, 114288. https://doi.org/10.1016/j.desal.2019.114288.
Li, H., Shi, W., Du, Q., Huang, S., Zhang, H., Zhou, R., Qin, X., 2022. Removal of high concentration Congo red by hydrophobic PVDF hollow fiber composite membrane coated with a loose and porous ZIF-71PVDF layer through vacuum membrane distillation. J. Ind. Text. 51, 7641S–7673S. https://doi.org/10.1177/1528083720967075.
Lian, B., Wang, Y., Le-Clech, P., Chen, V., Leslie, G., 2016. A numerical approach to module design for crossflow vacuum membrane distillation systems. J. Memb. Sci. 510, 489–496. https://doi.org/10.1016/j.memsci.2016.03.041.
Lim, W.J., Ooi, B.S., 2022. Applications of responsive hydrogel to enhance the water recovery via membrane distillation and forward osmosis: a review. J. Water Process Eng. 47, 102828 https://doi.org/10.1016/j.jwpe.2022.102828.
Lin, P.J., Yang, M.C., Li, Y.L., Chen, J.H., 2015. Prevention of surfactant wetting with agarose hydrogel layer for direct contact membrane distillation used in dyeing wastewater treatment. J. Memb. Sci. 475, 511–520. https://doi.org/10.1016/j.memsci.2014.11.001.
Liu, L., Xiao, Z., Liu, Y., Li, X., Yin, H., Volkov, A., He, T., 2021. Understanding the fouling/scaling resistance of superhydrophobic/omniphobic membranes in membrane distillation. Desalination 499, 114864. https://doi.org/10.1016/j.desal.2020.114864.
Liu, J., Lin, W., Ren, H., Albdoor, A.K., Hai, F.I., Ma, Z., 2022. Multi-objective optimization of a direct contact membrane distillation regenerator for liquid desiccant regeneration. J. Clean. Prod. 373 https://doi.org/10.1016/j.jclepro.2022.133736.
Loreti, L., Castro-mu, R., 2021. Ongoing progress on novel nanocomposite membranes for the separation of heavy metals from contaminated water. Chemosphere 270, 129421. https://doi.org/10.1016/j.chemosphere.2020.129421.
Lousada, M.E., Lopez Maldonado, E.A., Nthunya, L.N., Mosai, A., Antunes, M.L.P., Fraceto, L.F., Baigorria, E., 2023. Nanoclays and mineral derivates applied to pesticide water remediation. J. Contam. Hydrol. 259, 104264 https://doi.org/10.1016/j.jconhyd.2023.104264.
Ma, Q., Tong, L., Wang, C., Cao, G., Lu, H., Li, J., Liu, X., Feng, X., Wu, Z., 2022. Simulation and experimental investigation of the vacuum-enhanced direct membrane distillation driven by a low-grade heat source. Membranes 12. https://doi.org/10.3390/membranes12090842.
Madalosso, H.B., de Sousa Silva, R., Merlini, A., Battisti, R., Machado, R.A.F., Marangoni, C., 2021. Modeling and experimental validation of direct contact membrane distillation applied to synthetic dye solutions. J. Chem. Technol. Biotechnol. 96, 909–922. https://doi.org/10.1002/jctb.6599.
Mahlangu, T.O., Thwala, J.M., Mamba, B.B., D'Haese, A., Verliefde, A.R.D., 2015. Factors governing combined fouling by organic and colloidal foulants in cross-flow nanofiltration. J. Memb. Sci. 491, 53–62. https://doi.org/10.1016/j.memsci.2015.03.021.
Mahlangu, O.T., Nthunya, L.N., Motsa, M.M., Morifi, E., Richards, H., Mamba, B.B., 2023a. Fouling of high pressure-driven NF and RO membranes in desalination processes: mechanisms and implications on salt rejection. Chem. Eng. Res. Des. 199, 268–295. https://doi.org/10.1016/j.cherd.2023.09.037.
Mahlangu, O.T., Motsa, M.M., Hai, F.I., Mamba, B.B., 2023b. Role of membrane–solute affinity interactions in carbamazepine rejection and resistance to organic fouling by nano-engineered UF/PES membranes. Membranes 13. https://doi.org/10.3390/membranes13080744, 744.
Mahlangu, O.T., Nkambule, T.I., Mamba, B.B., Hai, F.I., 2024. Strategies for mitigating challenges associated with trace organic compound removal by high-retention membrane bioreactors (HR-MBRs). Npj Clean Water 7, 1–39. https://doi.org/10.1038/s41545-024-00313-w.
Mahmoud, A.S., Mostafa, M.K., Nasr, M., 2019. Regression model, artificial intelligence, and cost estimation for phosphate adsorption using encapsulated nanoscale zero-valent iron. Sep. Sci. Technol. 54, 13–26. https://doi.org/10.1080/01496395.2018.1504799.
Maity, S., Mishra, B., Nayak, K., Dubey, N.C., Tripathi, B.P., 2022. Zwitterionic microgel based anti(-bio)fouling smart membranes for tunable water filtration and molecular separation. Mater. Today Chem. 24, 100779 https://doi.org/10.1016/j.mtchem.2022.100779.
Makanjuola, O., Lalia, B.S., Hashaikeh, R., 2021. Thermoelectric heating and cooling for efficient membrane distillation. Case Stud. Therm. Eng. 28 https://doi.org/10.1016/j.csite.2021.101540.
Manzoor, K., Khan, S.J., Yasmeen, M., Jamal, Y., Arshad, M., 2022. Assessment of anaerobic membrane distillation bioreactor hybrid system at mesophilic and thermophilic temperatures treating textile wastewater. J. Water Process Eng. 46, 102603 https://doi.org/10.1016/j.jwpe.2022.102603.
Martínez, L., Rodríguez-Maroto, J.M., 2006. Characterization of membrane distillation modules and analysis of mass flux enhancement by channel spacers. J. Memb. Sci. 274, 123–137. https://doi.org/10.1016/j.memsci.2005.07.045.
Martínez-Díez, L., Vázquez-González, M.I., Florido-Díaz, F.J., 1998. Study of membrane distillation using channel spacers. J. Memb. Sci. 144, 45–56. https://doi.org/10.1016/S0376-7388(98)00024-6.
Mokhtar, N.M., Lau, W.J., Ismail, A.F., 2014a. The potential of membrane distillation in recovering water from hot dyeing solution. J. Water Process Eng. 2, 71–78. https://doi.org/10.1016/j.jwpe.2014.05.006.
Mokhtar, N.M., Lau, W.J., Ismail, A.F., 2014b. The potential of membrane distillation in recovering water from hot dyeing solution. J. Water Process Eng. 2, 71–78. https://doi.org/10.1016/j.jwpe.2014.05.006.
Mokhtar, N.M., Lau, W.J., Ismail, A.F., Youravong, W., Khongnakorn, W., Lertwittayanon, K., 2015. Performance evaluation of novel PVDF-Cloisite 15A hollow fiber composite membranes for treatment of effluents containing dyes and salts using membrane distillation. RSC Adv. 5, 38011–38020. https://doi.org/10.1039/c5ra00182j.
Mokhtar, N.M., Lau, W.J., Ismail, A.F., Kartohardjono, S., Lai, S.O., Teoh, H.C., 2016. The potential of direct contact membrane distillation for industrial textile wastewater treatment using PVDF-Cloisite 15A nanocomposite membrane. Chem. Eng. Res. Des. 111, 284–293. https://doi.org/10.1016/j.cherd.2016.05.018.
Mokhtara, N.M., Lau, W.J., Ismailb, A.F., Kartohardjonoc, S., Laid, S.O., Teoh, H.C., 2016. The potential of direct contact membrane distillation for industrial textile wastewater treatment using PVDF-Cloisite 15A nanocomposite. Chem. Eng. Res. Des. 111, 284–293. https://doi.org/10.1016/j.cherd.2016.05.018.
Mousavi, S.A., Arab Aboosadi, Z., Mansourizadeh, A., Honarvar, B., 2021a. Modification of porous polyetherimide hollow fiber membrane by dip-coating of Zonyl® BA for membrane distillation of dyeing wastewater. Water Sci. Technol. 83, 3092–3109. https://doi.org/10.2166/wst.2021.201.
Mousavi, S.A., Arab Aboosadi, Z., Mansourizadeh, A., Honarvar, B., 2021b. Modification of porous polyetherimide hollow fiber membrane by dip-coating of Zonyl® BA for

membrane distillation of dyeing wastewater. Water Sci. Technol. 83, 3092–3109. https://doi.org/10.2166/wst.2021.201.
Mozia, S., Morawski, A.W., Toyoda, M., Inagaki, M., 2008. Effectiveness of photodecomposition of an azo dye on a novel anatase-phase TiO2 and two commercial photocatalysts in a photocatalytic membrane reactor (PMR). Sep. Purif. Technol. 63, 386–391. https://doi.org/10.1016/j.seppur.2008.05.029.
Mpala, T.J., Etale, A., Richards, H., Nthunya, L.N., 2022. Biofouling phenomena in membrane distillation : mechanisms and mitigation strategies. Environ. Sci. Adv. 2, 39–54. https://doi.org/10.1039/d2va00161f.
Mpala, T.J., Serepa-dlamini, M.H., Etale, A., Richards, H., Nthunya, L.N., 2023a. Cellulose nanocrystal-mediated synthesis of silver nanoparticles via microwave assisted method for biofouling control in membrane distillation. Mater. Today Commun. 34, 105028 https://doi.org/10.1016/j.mtcomm.2022.105028.
Mpala, T.J., Richards, H., Etale, A., Mahlangu, O.T., Nthunya, L.N., 2023b. Carbon nanotubes and silver nanoparticles modification of PVDF membranes for improved seawater desalination in direct contact membrane distillation. Front. Membr. Sci. Technol. 2, 1–11. https://doi.org/10.3389/frmst.2023.1165678.
Mpala, T., Chimanlal, I., Richards, H., Etale, A., Nthunya, L.N., 2024. Hybrid membrane processes equipped with crystallization unit for a simultaneous recovery of freshwater and minerals from saline wastewater. In: Innov. Trends Remov. Refract. Pollut. From Pharm. Wastewater H. Elsevier, Netherlands, pp. 71–91. https://doi.org/10.1016/B978-0-323-99278-7.00010-9.
Musnicki, W.J., Lloyd, N.W., Phillips, R.J., Dungan, S.R., 2011. Diffusion of sodium dodecyl sulfate micelles in agarose gels. J. Colloid Interface Sci. 356, 165–175. https://doi.org/10.1016/j.jcis.2010.12.067.
Nadimi, M., Shahrooz, M., Wang, R., Yang, X., Duke, M.C., 2024. Process intensification with reactive membrane distillation: a review of hybrid and integrated processes. Desalination 573, 117182. https://doi.org/10.1016/j.desal.2023.117182.
Nguyen, T.A., Juang, R., 2013. Treatment of waters and wastewaters containing sulfur dyes : a review. Chem. Eng. J. 219, 109–117. https://doi.org/10.1016/j.cej.2012.12.102.
Noble, W.S., 2006. What is a support vector machine? Nat. Biotechnol. 24, 1565–1567. https://doi.org/10.1038/nbt1206-1565.
Nthunya, L.N., Gutierrez, L., Verliefde, A.R., Mhlanga, S.D., 2019a. Enhanced flux in direct contact membrane distillation using superhydrophobic PVDF nanofibre membranes embedded with organically modified SiO2 nanoparticles. J. Chem. Technol. Biotechnol. 94, 2826–2837. https://doi.org/10.1002/jcbt.6104.
Nthunya, L.N., Gutierrez, L., Derese, S., Edward, N., Verliefde, A.R., Mamba, B., Mhlanga, S.D., 2019b. A review of nanoparticle-enhanced membrane distillation membranes : membrane synthesis and applications in water treatment. Chem. Technol. Biotechnol 94, 2757–2771. https://doi.org/10.1002/jctb.5977.
Nthunya, L.N., Gutierrez, L., Khumalo, N., Derese, S., Mamba, B.B., Verliefde, A.R., Mhlanga, S.D., 2019c. Superhydrophobic PVDF nano fibre membranes coated with an organic fouling resistant hydrophilic active layer for direct-contact membrane distillation. Colloids Surfaces A 575, 363–372. https://doi.org/10.1016/j.colsurfa.2019.05.031.
Nthunya, L.N., Gutierrez, L., Khumalo, N., Derese, S., Mamba, B.B., Verliefde, A.R., Mhlanga, S.D., 2019d. Superhydrophobic PVDF nanofibre membranes coated with an organic fouling resistant hydrophilic active layer for direct-contact membrane distillation. Colloids Surfaces A Physicochem. Eng. Asp. 575, 363–372. https://doi.org/10.1016/j.colsurfa.2019.05.031.
Nthunya, L.N., Gutierrez, L., Nxumalo, E.N., Verliefde, A.R., Mhlanga, S.D., Onyango, M. S., 2020. f-MWCNTs/AgNPs-coated superhydrophobic PVDF nanofibre membrane for organic, colloidal, and biofouling mitigation in direct contact membrane distillation. J. Environ. Chem. Eng. 8, 103654 https://doi.org/10.1016/j.jece.2020.103654.
Nthunya, L.N., Bopape, M.F., Mahlangu, O.T., Mamba, B.B., Van der Bruggen, B., Quist-Jensen, C.A., Richards, H., 2022. Fouling, performance and cost analysis of membrane-based water desalination technologies: a critical review. J. Environ. Manag. 301, 113922 https://doi.org/10.1016/j.jenvman.2021.113922.
Nthunya, L.N., Pinier, J., Ali, A., Quist-jensen, C., Richards, H., 2024. Valorization of acid mine drainage into potable water and valuable minerals through membrane distillation crystallization. Sep. Purif. Technol. 334, 126084 https://doi.org/10.1016/j.seppur.2023.126084.
Ohale, P.E., Onu, C.E., Nwabanne, J.T., Aniagor, C.O., Okey-Onyesolu, C.F., Ohale, N.J., 2022. A comparative optimization and modeling of ammonia–nitrogen adsorption from abattoir wastewater using a novel iron-functionalized crab shell. Appl. Water Sci. 12, 1–27. https://doi.org/10.1007/s13201-022-01713-4.
Ounifi, I., Guesmi, Y., Ursino, C., Castro-Muñoz, R., Agougui, H., Jabli, M., Hafiane, A., Figoli, A., Ferjani, E., 2022. Synthesis and characterization of a thin-film composite nanofiltration membrane based on polyamide-cellulose acetate: application for water purification. J. Polym. Environ. 30, 707–718. https://doi.org/10.1007/s10924-021-02233-z.
Parakala, S., Moulik, S., Sridhar, S., 2019. Effective separation of methylene blue dye from aqueous solutions by integration of micellar enhanced ultrafiltration with vacuum membrane distillation. Chem. Eng. J. 375, 122015 https://doi.org/10.1016/j.cej.2019.122015.
Parani, S., Oluwafemi, O.S., 2021. Membrane distillation: recent configurations, membrane surface engineering, and applications. Membranes 11, 1–26. https://doi.org/10.3390/membranes11120934.
Pavithra, K.G., Jaikumar, S.K P.V., P, S.R, 2019. Removal of colorants from wastewater: a review on sources and treatment strategies. J. Ind. Eng. Chem. 75, 1–19. https://doi.org/10.1016/j.jiec.2019.02.011.
Pei, L., Liu, J., Wang, J., 2017. Study of dichlorotriazine reactive dye hydrolysis in siloxane reverse micro-emulsion. J. Clean. Prod. 165, 994–1004. https://doi.org/10.1016/j.jclepro.2017.07.185.
Petukhov, D.I., Johnson, D.J., 2024. Membrane modification with carbon nanomaterials for fouling mitigation: a review. Adv. Colloid Interface Sci. 327, 103140 https://doi.org/10.1016/j.cis.2024.103140.
Phattaranawik, J., Jiraratananon, R., Fane, A.G., 2003. Effects of net-type spacers on heat and mass transfer in direct contact membrane distillation and comparison with ultrafiltration studies. J. Memb. Sci. 217, 193–206. https://doi.org/10.1016/S0376-7388(03)00130-3.
Pichardo-romero, D., Garcia-arce, Z.P., Zavala-ram, A., Castro-muñoz, R., 2020. Current advances in biofouling mitigation in membranes for water treatment : an overview. Processes 8, 182, 10.3390/pr8020182.
Politano, A., Argurio, P., Di Profio, G., Sanna, V., Cupolillo, A., Chakraborty, S., Arafat, H.A., Curcio, E., 2017. Photothermal membrane distillation for seawater desalination. Adv. Mater. 29, 1–6. https://doi.org/10.1002/adma.201603504.
Qin, W., Xie, Z., Ng, D., Ye, Y., Ji, X., Gray, S., Zhang, J., 2018. Comparison of colloidal silica involved fouling behavior in three membrane distillation configurations using PTFE membrane. Water Res. 130, 343–352. https://doi.org/10.1016/j.watres.2017.12.002.
Rajkumar, D., Kim, J.G., 2006. Oxidation of various reactive dyes with in situ electro-generated active chlorine for textile dyeing industry wastewater treatment. J. Hazard Mater. 136, 203–212. https://doi.org/10.1016/j.jhazmat.2005.11.096.
Raman, C.D., Kanmani, S., 2016. Textile dye degradation using nano zero valent iron : a review. J. Environ. Manag. 177, 341–355. https://doi.org/10.1016/j.jenvman.2016.04.034.
Ramlow, H., Machado, R.A.F., Marangoni, C., 2017. Direct contact membrane distillation for textile wastewater treatment: a state of the art review. Water Sci. Technol. 76, 2565–2579. https://doi.org/10.2166/wst.2017.449.
Ramlow, H., Hugo, V., Correa, M., Antonio, R., Machado, F., Cristiane, A., Bierhalz, K., Marangoni, C., 2019a. Intensification of water reclamation from textile dyeing wastewater using thermal membrane technologies – performance comparison of vacuum membrane distillation and thermopervaporation. Chem. Eng. Process. Process Intensif. 146, 1–7. https://doi.org/10.1016/j.cep.2019.107695.
Ramlow, H., D'Ávila Kramer Cavalcanti, C., Machado, R.A.F., Krause Bierhalz, A.C., Marangoni, C., 2019b. Direct contact membrane distillation applied to colored reactive or disperse dye solutions. Chem. Eng. Technol. 42, 1045–1052. https://doi.org/10.1002/ceat.201800468.
Ramlow, H., Machado, R.A.F., Bierhalz, A.C.K., Marangoni, C., 2020. Direct contact membrane distillation applied to wastewaters from different stages of the textile process. Chem. Eng. Commun. 207, 1062–1073. https://doi.org/10.1080/00986445.2019.1640683.
Rauf, M.A., Hisaindee, S., 2013. Studies on solvatochromic behavior of dyes using spectral techniques. J. Mol. Struct. J. 1042, 45–56. https://doi.org/10.1016/j.molstruc.2013.03.050.
Ray, S.S., Bakshi, H.S., Dangayach, R., Singh, R., Deb, C.K., Ganesapillai, M., Chen, S.S., Purkait, M.K., 2020. Recent developments in nanomaterials-modified membranes for improved membrane distillation performance. Membranes 10, 1–29. https://doi.org/10.3390/membranes10070140.
Razaqpur, A.G., Wang, Y., Liao, X., Liao, Y., Wang, R., 2021. Progress of photothermal membrane distillation for decentralized desalination: a review. Water Res. 201, 117299 https://doi.org/10.1016/j.watres.2021.117299.
Reddy, A.S., Kalla, S., Murthy, Z.V.P., 2022. Textile wastewater treatment via membrane distillation. Environ. Eng. Res. 27, 1–16. https://doi.org/10.4491/eer.2021.228.
Roberto, Castro-Munoz, Agrawal, K.V., Coronas, J., 2020. Ultrathin permselective membranes: the latent way for efficient gas separation. RSC Adv. 10, 12653–12670. https://doi.org/10.1039/d0ra02254c.
Rovira, J., Domingo, J.L., 2019. Human health risks due to exposure to inorganic and organic chemicals from textiles: a review. Environ. Res. 168, 62–69. https://doi.org/10.1016/j.envres.2018.09.027.
Russo, F., Castro-muñoz, R., Galiano, F., Figoli, A., 2019. Unprecedented preparation of porous Matrimid ® 5218 membranes. J. Memb. Sci. 585, 166–174. https://doi.org/10.1016/j.memsci.2019.05.036.
Sadek, A.H., Mostafa, M.K., 2023. Preparation of nano zero-valent aluminum for one-step removal of methylene blue from aqueous solutions: cost analysis for scaling-up and artificial intelligence. Appl. Water Sci. 13, 1–23. https://doi.org/10.1007/s13201-022-01837-7.
Said, I.A., Chomiak, T., Floyd, J., Li, Q., 2020. Sweeping gas membrane distillation (SGMD) for wastewater treatment, concentration, and desalination: a comprehensive review. Chem. Eng. Process. - Process Intensif. 153, 107960 https://doi.org/10.1016/j.cep.2020.107960.
Salehi, E., Castro-mu, R., 2023. Zeolitic imidazolate framework (ZIF-8) modified cellulose acetate NF membranes for potential water treatment application, 299. https://doi.org/10.1016/j.carbpol.2022.120230.
Samsami, S., Mohamadi, M., Sarrafzadeh, M.H., Rene, E.R., Firoozbahr, M., 2020. Recent advances in the treatment of dye-containing wastewater from textile industries: overview and perspectives. Process Saf. Environ. Prot. 143, 138–163. https://doi.org/10.1016/j.psep.2020.05.034.
Sathishkumar, V.E., Ramu, A.G., Cho, J., 2023. Machine learning algorithms to predict the catalytic reduction performance of eco-toxic nitrophenols and azo dyes contaminants (Invited Article). Alex. Eng. J. 72, 673–693. https://doi.org/10.1016/j.aej.2023.04.007.
Serra, C., Kogevinas, M., Silverman, D.T., Turuguet, D., Tardon, A., Carrato, A., Castan, G., Fernandez, F., Stewart, P., Benavides, F.G., 2008. Work in the textile industry in Spain and bladder cancer. Occup. Environ. Med. 65, 552–559. https://doi.org/10.1136/oem.2007.035667.
Shahu, V.T., Thombre, S.B., 2019. Air gap membrane distillation: a review. J. Renew. Sustain. Energy 11. https://doi.org/10.1063/1.5063766.

shekhi Abadi, P.G., Irani, M., Rad, L.R., 2023. Mechanisms of the removal of the metal ions, dyes, and drugs from wastewaters by the electrospun nanofiber membranes. J. Taiwan Inst. Chem. Eng. 143, 104625 https://doi.org/10.1016/j.jtice.2022.104625.

Shi, W., Li, T., Tian, Y., Li, H., Fan, M., Zhang, H., Qin, X., 2022. An innovative hollow fiber vacuum membrane distillation-crystallization (VMDC) coupling process for dye house effluent separation to reclaim fresh water and salts. J. Clean. Prod. 337, 130586 https://doi.org/10.1016/j.jclepro.2022.130586.

Shirazi, M.M.A., Kargari, A., 2015. A review on applications of membrane distillation (MD) process for wastewater treatment. J. Membr. Sci. Res. 1, 101–112.

Shirazi, M.M.A., Kargari, A., Tabatabaei, M., 2014. Evaluation of commercial PTFE membranes in desalination by direct contact membrane distillation. Chem. Eng. Process. Process Intensif. 76, 16–25. https://doi.org/10.1016/j.cep.2013.11.010.

Shirazi, M.M.A., Bazgir, S., Meshkani, F., 2020a. A dual-layer, nanofibrous styrene-acrylonitrile membrane with hydrophobic/hydrophilic composite structure for treating the hot dyeing effluent by direct contact membrane distillation. Chem. Eng. Res. Des. 164, 125–146. https://doi.org/10.1016/j.cherd.2020.09.030.

Shirazi, M.M.A., Bazgir, S., Meshkani, F., 2020b. A novel dual-layer, gas-assisted electrospun, nanofibrous SAN4-HIPS membrane for industrial textile wastewater treatment by direct contact membrane distillation (DCMD). J. Water Process Eng. 36, 101315 https://doi.org/10.1016/j.jwpe.2020.101315.

Silva, R. de S., Ramlow, H., Cavalcanti, C.D.Á.K., Valle, C., Machado, R.A.F., Marangoni, C., 2020. Steady state evaluation with different operating times in the direct contact membrane distillation process applied to water recovery from dyeing wastewater. Sep. Purif. Technol. 230, 2–10. https://doi.org/10.1016/j.seppur.2019.115892.

Silva, R. de S., Ramlow, H., Santos, B. de C., Madalosso, H.B., Machado, R.A.F., Marangoni, C., 2021a. Membrane Distillation: experimental evaluation of Liquid Entry Pressure in commercial membranes with textile dye solutions. J. Water Process Eng. 44, 102339 https://doi.org/10.1016/j.jwpe.2021.102339.

Silva, R. de S., Cavalcanti, C.D.Á.K., Valle, C., Machado, R.A.F., Marangoni, C., 2021b. Understanding the effects of operational conditions on the membrane distillation process applied to the recovery of water from textile effluents. Process Saf. Environ. Prot. 145, 285–292. https://doi.org/10.1016/j.psep.2020.08.022.

Singh, Z., Chadha, P., 2016. Textile industry and occupational cancer. J. Occup. Med. Toxicol. 11, 1–6. https://doi.org/10.1186/s12995-016-0128-3.

Song, L., Li, B., Sirkar, K.K., Gilron, J.L., 2007. Direct contact membrane distillation-based desalination: novel membranes, devices, larger-scale studies, and a model. Ind. Eng. Chem. Res. 46, 2307–2323. https://doi.org/10.1021/ie0609968.

Su, C.X.H., Low, L.W., Teng, T.T., Wong, Y.S., 2016. Combination and hybridisation of treatments in dye wastewater treatment: a review. J. Environ. Chem. Eng. 4, 3618–3631. https://doi.org/10.1016/j.jece.2016.07.026.

Subramanian, Y., Gajendiran, J., Veena, R., Azad, A.K., Sabarish, V.C.B., Muhammed Ali, S.A., Kumar, A., Gubendiran, R.K., 2023. Structural, photoabsorption and photocatalytic characteristics of BiFeO3-WO3 nanocomposites: an attempt to validate the experimental data through SVM-based artificial intelligence (AI). J. Electron. Mater. 52, 2421–2431. https://doi.org/10.1007/s11664-022-10188-7.

Summers, E.K., Arafat, H.A., Lienhard V, J.H., 2012. Energy efficiency comparison of single-stage membrane distillation (MD) desalination cycles in different configurations. Desalination 290, 54–66. https://doi.org/10.1016/j.desal.2012.01.004.

Suresh, R., Rajendran, S., Gnanasekaran, L., Show, P.L., Soto-moscoso, M., 2023. Modified poly(vinylidene fluoride) nanomembranes for dye removal from water – a review. Chemosphere 322, 138152. https://doi.org/10.1016/j.chemosphere.2023.138152.

Tai, Z.S., Othman, M.H.D., Koo, K.N., Jaafar, J., 2023. Critical review on membrane designs for enhanced flux performance in membrane distillation. Desalination 553, 116484. https://doi.org/10.1016/j.desal.2023.116484.

Teoh, M.M., Bonyadi, S., Chung, T.S., 2008. Investigation of different hollow fiber module designs for flux enhancement in the membrane distillation process. J. Memb. Sci. 311, 371–379. https://doi.org/10.1016/j.memsci.2007.12.054.

Tewodros, B.N., Yang, D.R., Park, K., 2022. Design parameters of a direct contact membrane distillation and a case study of its applicability to low-grade waste energy. Membranes 12, 1–31. https://doi.org/10.3390/membranes12121279.

Tian, R., Gao, H., Yang, X.H., Yan, S.Y., Li, S., 2014. A new enhancement technique on air gap membrane distillation. Desalination 332, 52–59. https://doi.org/10.1016/j.desal.2013.10.016.

Tolentino Filho, C.M., Silva, R. de S., Cavalcanti, C.D.Á.K., Granato, M.A., Machado, R.A.F., Marangoni, C., 2022. Membrane distillation for the recovery textile wastewater: influence of dye concentration. J. Water Process Eng. 46, 102611 https://doi.org/10.1016/j.jwpe.2022.102611.

Tournis, I., Tsiourvas, D., Sideratou, Z., Boutsika, L.G., Papavasiliou, A., Boukos, N.K., Sapalidis, A.A., 2022. Superhydrophobic nanoparticle-coated PVDF-HFP membranes with enhanced flux, anti-fouling and anti-wetting performance for direct contact membrane distillation-based desalination. Environ. Sci. Water Res. Technol. 8, 2373–2380. https://doi.org/10.1039/d2ew00407k.

Ullah, R., Khraisheh, M., Esteves, R.J., McLeskey, J.T., AlGhouti, M., Gad-el-Hak, M., Vahedi Tafreshi, H., 2018. Energy efficiency of direct contact membrane distillation. Desalination 433, 56–67. https://doi.org/10.1016/j.desal.2018.01.025.

Winter, D., Koschikowski, J., Wieghaus, M., 2011. Desalination using membrane distillation: experimental studies on full scale spiral wound modules. J. Memb. Sci. 375, 104–112. https://doi.org/10.1016/j.memsci.2011.03.030.

Winter, D., Koschikowski, J., Gross, F., Maucher, D., Düver, D., Jositz, M., Mann, T., Hagedorn, A., 2017. Comparative analysis of full-scale membrane distillation contactors - methods and modules. J. Memb. Sci. 524, 758–771. https://doi.org/10.1016/j.memsci.2016.11.080.

Wu, X., Ma, S., Ng, D., Acharya, D., Fan, L., Xie, Z., 2024. Enhancing water recovery through integrated graphene oxide-modified forward osmosis and membrane distillation for real textile wastewater treatment. J. Environ. Chem. Eng. 12, 112512 https://doi.org/10.1016/j.jece.2024.112512.

Xiao, H., Zhao, T., Li, C., Li, M., 2017. Eco-friendly approaches for dyeing multiple type of fabrics with cationic reactive dyes. J. Clean. Prod. 165, 1499–1507. https://doi.org/10.1016/j.jclepro.2017.07.174.

Xie, S., Du, J., Huang, X., Gu, A., Fang, S., Liu, R., Zou, D., Lin, J., Xie, M., Zhao, S., Ye, W., 2023. Water recovery from highly saline dye wastewater by membrane distillation using a superhydrophobic SiO2/PVDF membrane. ACS ES T Water 3, 1893–1901. https://doi.org/10.1021/acsestwater.2c00519.

Xu, H., Xiao, K., Wang, X., Liang, S., Wei, C., Wen, X., Huang, X., 2020. Outlining the roles of membrane-foulant and foulant-foulant interactions in organic fouling during microfiltration and ultrafiltration: a mini-review. Front. Chem. 8, 1–14. https://doi.org/10.3389/fchem.2020.00417.

Yadav, A., Patel, R.V., Labhasetwar, P.K., Shahi, V.K., 2021a. Novel MIL101(Fe) impregnated poly(vinylidene fluoride-co-hexafluoropropylene) mixed matrix membranes for dye removal from textile industry wastewater. J. Water Process Eng. 43, 102317 https://doi.org/10.1016/j.jwpe.2021.102317.

Yadav, A., Sharma, P., Panda, A.B., Shahi, V.K., 2021b. Photocatalytic TiO2 incorporated PVDF-co-HFP UV-cleaning mixed matrix membranes for effective removal of dyes from synthetic wastewater system via membrane distillation. J. Environ. Chem. Eng. 9, 105904 https://doi.org/10.1016/j.jece.2021.105904.

Yadav, A., Patel, R.V., Singh, C.P., Labhasetwar, P.K., Shahi, V.K., 2022. Experimental study and numerical optimization for removal of methyl orange using polytetrafluoroethylene membranes in vacuum membrane distillation process. Colloids Surfaces A Physicochem. Eng. Asp. 635, 1–14. https://doi.org/10.1016/j.colsurfa.2021.128070.

Yan, Z., Jiang, Y., Liu, L., Li, Z., Chen, X., Xia, M., Fan, G., Ding, A., 2021. Membrane distillation for wastewater treatment: a mini Review. Water 13, 1–28. https://doi.org/10.3390/w13243480.

Yan, Z., Chen, X., Bao, S., Chang, H., Liu, H., Fan, G., Wang, Q., Fu, X., Qu, F., Liang, H., 2022. Integration of in situ Fenton-like self-cleaning and photothermal membrane distillation for wastewater treatment via Co-MoS2/CNT catalytic membrane. Sep. Purif. Technol. 303, 122207 https://doi.org/10.1016/j.seppur.2022.122207.

Yang, X., Wang, R., Fane, A.G., Tang, C.Y., Wenten, I.G., 2013. Membrane module design and dynamic shear-induced techniques to enhance liquid separation by hollow fiber modules: a review. Desalin. Water Treat. 51, 3604–3627. https://doi.org/10.1080/19443994.2012.751146.

Yang, G., Zhang, J., Peng, M., Du, E., Wang, Y., Shan, G., Ling, L., Ding, H., Gray, S., Xie, Z., 2021. A mini review on antiwetting studies in membrane distillation for textile wastewater treatment. Processes 9, 1–16. https://doi.org/10.3390/pr9020243.

Yang, H., Yu, X., Liu, J., Tang, Z., Huang, T., Wang, Z., Zhong, Y., Long, Z., Wang, L., 2022a. A concise review of theoretical models and numerical simulations of membrane fouling. Water 14, 3537. https://doi.org/10.3390/w14213537.

Yang, S., Abdalkareem Jasim, S., Bokov, D., Chupradit, S., Nakhjiri, A.T., El-Shafay, A.S., 2022b. Membrane distillation technology for molecular separation: a review on the fouling, wetting and transport phenomena. J. Mol. Liq. 349, 118115 https://doi.org/10.1016/j.molliq.2021.118115.

Yun, Y., Ma, R., Zhang, W., Fane, A.G., Li, J., 2006. Direct contact membrane distillation mechanism for high concentration NaCl solutions. Desalination 188, 251–262. https://doi.org/10.1016/j.desal.2005.04.123.

Zamidi, M., Martin-gil, V., Supinkova, T., Lambert, P., 2021. Novel MMM using CO2 selective SSZ-16 and high-performance 6FDA- polyimide for CO2/CH4 separation. Sep. Purif. Technol. 254, 117582 https://doi.org/10.1016/j.seppur.2020.117582.

Zamidi, M., Malankowska, M., Castro-mu, R., 2022. A new relevant membrane application: CO2 direct air capture (DAC). Chem. Eng. J. 446, 137047 https://doi.org/10.1016/j.cej.2022.137047.

Zaragoza, G., Ruiz-Aguirre, A., Guillén-Burrieza, E., 2014. Efficiency in the use of solar thermal energy of small membrane desalination systems for decentralized water production. Appl. Energy 130, 491–499. https://doi.org/10.1016/j.apenergy.2014.02.024.

Zhang, W., Ding, L., 2015. Investigation of membrane fouling mechanisms using blocking models in the case of shear-enhanced ultrafiltration. Sep. Purif. Technol. 141, 160–169. https://doi.org/10.1016/j.seppur.2014.11.041.

Zhang, S., Ma, W., Ju, B., Dang, N., Zhang, M., 2005. Continuous dyeing of cationised cotton with reactive dyes Coloration Technology. Color. Technol. 121, 183–186.

Zhang, J., De Li, J., Duke, M., Hoang, M., Xie, Z., Groth, A., Tun, C., Gray, S., 2013. Influence of module design and membrane compressibility on VMD performance. J. Memb. Sci. 442, 31–38. https://doi.org/10.1016/j.memsci.2013.04.028.

Zhang, L., Sha, C., Li, B., Wang, W., 2023. Investigation of utilizing carbonized lotus root as photothermal material in the solar steam generation system. Energy Sources, Part A Recover. Util. Environ. Eff. 45, 3359–3368. https://doi.org/10.1080/15567036.2023.2196953.